ISTITUTO SUPERIORE DI SANITÀ

Methodologies and measurement devices for an effective functional assessment of the diabetic foot

Claudia Giacomozzi

Laboratorio di Ingegneria Biomedica

ISSN 1123-3117

Rapporti ISTISAN
03/31

Istituto Superiore di Sanità
Methodologies and measurement devices for an effective functional assessment of the diabetic foot.
Claudia Giacomozzi
2003, ii, 61 p. Rapporti ISTISAN 03/31

Diabetes mellitus is characterised by metabolic abnormalities which produce damaging events in almost every tissue and organ. One of the most serious consequences of compromised motor control of gait are plantar ulcers, hard to heal, highly recurrent, and which usually lead to amputation. Unfortunately, the prevention of diabetic ulcers is still poorly effective. A bioengineering approach was used in this study to gain deeper knowledge in the functional alterations of the foot-ankle complex. Measurement equipments and methodologies which are typical of gait analysis were setup and specialised for the purpose. A wide clinical investigation was conducted on 61 diabetics and 21 healthy volunteers. The final biomechanical contribution was a functional model which explains the main mechanical causes of dangerous plantar pressures, serious functional impairments, and changes in locomotor strategies. The clinical target of this study was the identification of specific tools for a more effective foot screening and ulcer prevention.
Key words: Diabetes, Plantar ulcers, Biomechanics, Gait analysis, Functional assessment

Istituto Superiore di Sanità
Metodologie e strumentazione per un'efficace valutazione funzionale del piede diabetico.
Claudia Giacomozzi
2003, ii, 61 p. Rapporti ISTISAN 03/31 (in inglese)

Il diabete mellito è caratterizzato da alterazioni metaboliche che danneggiano quasi tutti i tessuti e gli organi umani. Una delle conseguenze più serie della compromissione del controllo motorio del cammino sono le ulcere plantari, di difficile guarigione, altamente ricorrenti, spesso causa di amputazione. Sfortunatamente, la prevenzione delle ulcere diabetiche è ancora poco efficace. Nel presente studio si è seguito un approccio bioingegneristico per approfondire le conoscenze delle alterazioni funzionali del complesso caviglia-piede. Allo scopo sono stati specializzati strumenti e metodi tipici dell'analisi del cammino. È stata condotta un'ampia indagine clinica su 61 pazienti e 21 volontari sani. Il contributo biomeccanico finale è stato un modello funzionale che giustifica le principali cause meccaniche all'origine di pericolose pressioni plantari, serie limitazioni funzionali, e cambiamenti di strategie deambulatorie. Obiettivo clinico dello studio è stata l'identificazione di strumenti di analisi specifici e più efficaci per lo screening del piede e la prevenzione delle ulcere.
Parole chiave: Diabete, Ulcere plantari, Biomeccanica, Analisi del cammino, Valutazione funzionale

Acknowledgements: Velio Macellari for scientific revision and Monica Brocco for linguistic revision.

The part of the present study related to the design of the ankle measurement device was partly sponsored by INAIL (Istituto Nazionale per l'Assicurazione contro gli Infortuni sul Lavoro, Italian national institute of assurance for injured workers).

Per informazioni su questo documento scrivere a: claudia.giacomozzi@iss.it

Il rapporto è accessibile online dal sito di questo Istituto: www.iss.it/pubblicazioni.

Presidente dell'Istituto Superiore di Sanità e Direttore responsabile: *Enrico Garaci*
Registro della Stampa - Tribunale di Roma n. 131/88 del 1° marzo 1988

Redazione*: Paola De Castro* e *Sandra Salinetti*
La responsabilità dei dati scientifici e tecnici è dei singoli autori.

INDICE

DIABETES AND THE FOOT-ANKLE COMPLEX

Diabetes mellitus is the most common endocrine disease and is characterised by metabolic abnormalities and long-term complications. The disease is widely spread in the western world, although the true frequency is difficult to ascertain because of differing standards of diagnosis. As the life expectancy of the populations grows, the number of diabetic patients increases. Several distinct diabetic syndromes have been delineated accordingly to the different clinical criteria and pathogenesis. However, the different syndromes are characterised by the common sign of hyperglycemia. Hyperglycemia causes the main manifestations of symptomatic diabetes mellitus (polyuria, polydipsia and polyphagia) and promotes glycosilation of proteins and the consequent accumulation of advanced glycosilation end-products in tissues (1). Damaging events are then produced in almost every tissue and organ. Complications of diabetic origin have been assessed in terms of retinopathy, nephropathy, peripheral neuropathy, tendinopathy, cardiovascular diseases, difficulty in wounds healing, pathologies of pregnancy, and so on.

Diabetic peripheral neuropathy is responsible for sensory deficiencies of the most distal parts of the body, namely hands and feet (2-3). In particular, the motor control of gait is compromised by the diminished feedback from the somatosensory system (4). Nerve degeneration may also cause myopathic changes, muscle atrophy and weakness, and the resulting motor neuropathies may further compromise the performance of gait (5).

Plantar ulcers should be considered one of the most serious consequences of gait alteration due to diabetic peripheral neuropathy. The recurrence rate of these hard-to-heal wounds is very high, usually entails the amputation of the minor or major foot joints. Epidemiologic data are still not available in Italy, but in the United States 56% to 83% of amputations occur in people with diabetes, peripheral sensory neuropathy and neuropathic ulceration. About 15% of diabetic patients will likely develop foot ulcers, and approximately 15% to 20% of these ulcers will result in lower-extremity amputation. These data easily explain the great interest in the treatment of the diabetic foot and the prevention of ulcers (2).

A wide scientific documentation has been already produced, that deals with diabetic neuropathy, both of sensory and motor origin (6-12). Accurate research projects have been conducted so far aimed at investigating and characterising all known and potential causes of the ulceration process of the plantar surface. Unfortunately, the prevention of neuropathic ulcers is poorly effective, as pitted against the human and economic efforts of the scientific community. Cavanagh made an interesting review about the current developments in the biomechanics of the diabetic foot (13), in which a critical role is ascribed to the mechanical stress of the soft tissues under the metatarsal heads in the pathogenesis of the neuropathic ulcer. The authors of the review encouraged the investigation and quantification of as many mechanical factors as possible, and suggested to focus on: the identification of a plantar-pressure risk threshold; the measurement of shear stress during walking; the association between foot deformity and plantar pressures; the characterisation of the role of calluses; the association between Achilles tendon lengthening and decreased plantar pressure; the measurement of muscular weakness at the ankle.

The main aim of the present study is to give a biomechanical contribution to the definition of a functional model of the diabetic foot. The term “functional” means that measurement equipments, protocols and methodologies were all designed to characterise the main functional alterations of the foot itself, of the ankle articular complex, and the main leg muscles acting on them. The final result should be a better comprehension of the biomechanical causes which

determine elevated, dangerous plantar pressures, serious functional impairments during gait, and eventual changes of locomotor strategies.

This specific study originated from the hypothesis that several factors, thought as either primary or secondary consequences of glycosilation, may contribute to the ulceration of the diabetic neuropathic foot according to linear (superimposition of the effects) or more complex laws. Under this hypothesis, it seemed extremely helpful to analyse and discuss the effect of each factor as if it were the only and independent cause of ulceration. The observation that the numerous investigated factors may combine in several possible ways, gave reason of the high variability of the conditions under which the ulceration process begins, and the derived difficulty in determining effective (sensible and specific) risk thresholds, but, most importantly, it explained why mild alterations of more factors, none of which dangerous in itself, determine highly impairing situations when occurring simultaneously.

The proposed functional model accounts for all those functional blocks whose alterations with respect to age-matched control groups may be ascribed to locomotor pathologies directly related to diabetes. More precisely, three main functional blocks have been identified: i) articular mobility of ankle, subtalar and 1st metatarso-phalangeal joints; ii) muscular functionality of main ankle plantar and dorsal flexor muscles; iii) thickening of tendinous and ligamentous structures of foot and ankle, with special attention to Achilles tendon and plantar fascia.

From a clinical point of view, the study was primarily aimed at designing rehabilitation processes that should prevent the onset of plantar ulcers. This would entail a better knowledge of the functionality of the whole foot-ankle complex, and the quantification of the contribution of each functional block to the performance of gait. A second, useful clinical target of this study was the identification of few parameters, easily measurable during ambulatory foot screening, whose variations reflect some of the examined functional alterations. This could supply the clinicians with sensible and specific tools for a more effective ulcer prevention.

Foot-floor interaction

Abnormal plantar pressures are considered to play a major role in the pathogenesis of neuropathic ulcers in the diabetic foot (14-18).

In 1975 Stokes noticed that ulcers develop in the sites of the highest load, such as the plantar surfaces of the metatarsal heads and toes (14). Since then, many other authors have described “high plantar pressures” in the diabetic neuropathic foot and their relationship with ulcer development (15-18).

However, several authors have also formulated the hypothesis that the increased plantar pressure alone, and thus the increased normal stress, is not the only determinant of tissue breakdown (13,19-20), and that tangential stress should also be considered. The hypothesis was mainly based on the following grounds:

1. the ulcer risk threshold, in terms of plantar pressure peaks, has not yet been clearly established (there is a wide overlap between plantar pressure peaks distribution in healthy people and in neuropathic patients with ulcers) (21-22);
2. although callus formation appears to have a mechanical etiology, not all areas of high plantar pressures develop callus (the exact mechanical stimulus for callus formation is still unclear) (23);
3. not all ulcers develop at highest-pressure sites (24).

Using pressure platforms, many authors have quantitatively assessed the vertical component of the Ground Reaction Force (GRF) that originates from the foot-to-floor interaction during

gait, but, due to the technical characteristics of these devices, they could infer nothing about the two horizontal components of this force, namely the anterior-posterior and the medio-lateral component.

Conversely, the dynamometric platforms measure all three GRF components. The main drawback is that they only record the resultant of GRF measured under the whole foot; this means that these devices do not extrapolate forces acting on specific foot subareas. Moreover, they do not show the foot position on the platform, which prevents the identification of the above subareas and the computation of their contribution to total GRF (25-26).

The use of a piezo-dynamometric integrated platform, obtained by superimposing a pressure platform over a force platform (27), allowed the estimation of the three components of GRF expressed by specific selected foot subareas (28).

Thus, aim of this part of the present study was to describe the tangential and vertical forces for total foot and selected subareas of interest in diabetic patients, with or without neuropathy or previous ulceration, and to compare them with those recorded from control subjects.

A further step in the analysis of foot-floor interaction came from the observation that high pressures are only the last effect of a chain of changes and adaptations of deambulatory strategies in the presence of diabetes and peripheral neuropathy. Factors like limited joint mobility, tendinopathy and muscle weakness may influence not only the foot loading but, more widely, the whole performance of the lower limb. Specific changes thus appear in the way neuropathic patients do manage their gait, and few authors have suggested that patients with peripheral neuropathy control their walking by shifting their strategy from an ankle strategy to a hip strategy. Peculiar loading patterns of the diabetic neuropathic foot have then been hypothesised, observed, and even imposed in the attempt of reducing hyperpressure under the forefoot of patients at risk of ulceration or at risk of recurrence (29-30).

Of all the kinetic parameters that characterise foot-floor interaction during gait, Centre Of Pressure (COP) – i.e. the point of application of the GRF – seemed the most suitable and effective variable to account for significant changes in the kinematics and kinetics of the anatomical structures of the foot and of those acting on it. The importance of COP pattern alterations during gait has been widely asserted in the specialized literature (31-37). Since COP monitors, frame by frame, the foot-floor interaction, the succession of COP instantaneous positions accounts for the displacement of load throughout the foot during the stance phase of a walking cycle.

The aim of the present study was to quantify the changes in the loading patterns and to monitor the excursion of the COP during gait. Special attention was paid to loading times of selected foot subareas, anterior-posterior and medio-lateral COP excursions, COP integral along the longitudinal axis of the foot (38).

Joint mobility and muscular functionality of the foot-ankle complex

Besides the large amount of experimental data related to the analysis of foot-floor interaction, the specialised literature also reports clinical observations, hypotheses, modelling and *in vivo* or *in vitro* measurements aimed at better understanding the biomechanical changes which determine the change of locomotor strategy and the development of a “functional” flat foot in diabetic patients with peripheral neuropathy. Several authors have dealt with the reduction of the active or passive angular excursion at the ankle articular complex and at the metatarso-phalangeal joints. From the measurements made with varying accuracy and under

different loading conditions, a general trend was observed in which the angular range of motion significantly reduced especially with respect to the sagittal plane (flexion-extension movements). Hypotheses were presented about possible alterations in the structure and elasticity of cartilages and articular capsules, which might interfere with joint mobility. A large number of studies have also been conducted in order to investigate the role of potential muscular deficits. Muscles of the lower leg, namely the plantar and dorsal flexors of the ankle complex, and muscle-tendon links have been analysed both *in vivo* and *in vitro*, and several 2D or 3D models have been proposed to explain their function under normal or pathologic conditions. Most of the *in vivo* studies analysed the muscle compartments while working under isokinetic conditions. This means that the peak torques were measured during the performance of rapid movements (usually 60°/s), thus involving the recruitment and the performance of fast fibers only. The patient worked under loaded conditions, and the muscular mass played an important role in the final result.

The need arose, then, for a more accurate and complete quantification of the mobility of the ankle articular complex in all the planes of the anatomical reference system, and of its muscular functionality under well controlled conditions.

From a general biomechanical point of view, various models have been conceived to quantitatively analyse foot motion with respect to the shank, and related dynamics in terms of forces and torques exerted on the foot by the muscular groups of the lower leg (39-40). These works were based on *in vitro* and *in vivo* experiments. Most of the *in vivo* research methods are invasive and only give a partial, simplified description of the articular complex, which is often modelled as a two-hinge joints chain (41-43).

Even though many important issues still need to be discussed, several features have been generally observed and discussed elsewhere (44). One of the most important finding was the changing of the instantaneous axis of rotation of the ankle (tibio-talar) joint, thus suggesting that the hinge joint complex is an oversimplification for the ankle joint. A close interaction was also claimed between the geometry of the ligaments and the shape of the articular surfaces in guiding and stabilising motion at the ankle joint. As for the motion of the subtalar joint, even greater variability was found among the published experiments, mainly depending on conditions and methods of examination. The orientation of its axis of rotation was frequently discussed. As reported by Leardini (44), several authors described the subtalar joint as a hinge joint, with an oblique axis running approximately from antero-medio-superior to postero-latero-inferior direction (42, 45-46).

Thus the motion of the calcaneus with respect to the talus involves rotations in all three anatomical planes. Further studies demonstrated the changing positions and orientations for this axis, thus more complex models have been proposed, which consider the multiaxial nature of the joints (47). When considering the whole ankle complex, the “closed spatial kinematic chain” principle was described by Huson. On the basis of this principle, any movement of any tarsal bone occurs according to a fixed and coupled pattern which allows only one Degree Of Freedom (DOF), and polyaxial joints should replace single axis of rotation joints. Ligaments play an important role in the guidance of motion, since the articular contact showed incongruency during movement (48).

The complex mechanical coupling between ankle and subtalar joints has also been compared with that of a universal-joint type of linkage, which is able to transfer prono-supination of the calcaneus to tibial internal-external rotation and vice-versa (49). Ankle complex has been also recently modelled as a system with two monocentric, single DOF hinge joints (43). Alternatively, the kinematics of these joints has been modelled as an equivalent screw axis that provides a full six DOF (50). Such representations provide information of the entire motion, but little information for normal or pathological motion of either joint.

Studies on the kinematics of the ankle joint have shown that during the loaded movement of the foot with respect to the shank, it is difficult to predict the relative movements of the parts of the ankle complex (51). Approximated models can be built by assuming that the articular axes are coincident in a fixed point located in the middle of the segment which connects the tips of the tibial and fibular malleoli (52-54). However, the development of these models is very difficult, and simpler models based on fixed hinges or spherical joints do not yield reality-fitting representations of the ankle joint complex (54-55).

Moreover, it has been observed that the ankle and the subtalar joint are not subject to independent regulation, thus the resultant combined movement might be of greater functional value than the separate components (56).

Further difficulties arise in *in vivo* static and dynamic analyses, owing to the indeterminacy of the resultant force exerted on the foot. On the other hand, the knowledge of the force and torque components along and around the articular axes is important to estimate the inner stresses of the single parts of the complex. This bulk of information could be very useful for various applications, such as the design of prostheses or the definition of rehabilitating therapies, and is essential for a deeper knowledge of the functional impairments derived from the onset of diabetes and further worsened by peripheral sensory and motor neuropathy.

For this purpose a tool was developed at the Laboratory of Biomedical Engineering of the Istituto Superiore di Sanità (ISS; the Italian National Institute of Health, Rome), for the complete description of the kinematics and the isometric loading of the ankle joints (talo-crural and subtalar joints) under different conditions (57). Non-invasive, *in vivo* experiments can be conducted with this experimental apparatus. The device allows six DOF, three rotations and three translations; 6 transducers allow to fully describe the movement of the foot with respect to the shank. Then, for every position of the ankle articular complex, it is possible to evaluate the torques around the three articular axes, related to the movements of flexion-extension (in the sagittal plane), internal-external rotation (in the transversal plane), and foot inversion-eversion (in the frontal plane). The characterisation of the articular complex can be completed by integrating the proposed device with advanced superficial electromyographic techniques and electrical stimulation. In this way the functionality of the main muscular compartments of the lower leg can be assessed in both mechanical and myoelectrical terms. In the present study, surface EMG arrays electrodes (8 contacts, interelectrode distance 10 mm) were applied to the main superficial leg muscles, namely tibialis anterior, peroneus longus, and gastrocnemii.

The device might also be successfully employed to implement and monitor preventive, rehabilitative processes. The complete measurement system was preliminarily tested on healthy subjects and it proved to be reliable, precise and accurate, robust, and to have high repeatability.

Functionality of tendinous and ligamentous structures of the foot-ankle complex

As already reported, diabetes results in tissue damage due to protein glycosilation, and diabetic peripheral neuropathy leads to nerve degeneration and reduced muscle innervation. Related effects on the tendinous structures of hands and feet have been clinically observed, and studies reported on the structural changes in soft tissues. However, it is not known whether soft tissue abnormalities contribute to the increased plantar pressure and therefore to the risk of ulceration (58); whether they are related to observed foot deformities; whether they have a role in the functional impairment of foot joints, especially the 1st metatarso-phalangeal joint.

As stated before, it seemed helpful to analyse and discuss the effect of each factor as if it were the only and independent cause of pathogenesis of neuropathic ulcers. Thus, this part of the study only focused on the characterisation of the functional alterations of the anatomic and biomechanical unit formed by Achilles tendon, plantar fascia and metatarso-phalangeal joints, regarded as a direct consequence of thickening of tendineous and ligamentous tissues.

Achilles tendon alone has been widely investigated, and its role in determining limited joint mobility at the ankle joint (joint between tibia and talus) and in contributing to hyperpressure under the metatarsal heads has been discussed and documented (59-61). The effects of Achilles tendon lengthening on pressure relief have also been reported (62-64), even though doubts have been raised about the long-term effectiveness of this method (64).

Being a soft tissue, Achilles tendon is made of connective tissue, white and dense, arranged in parallel bundles of collagenous fibers containing relatively few fibroblast cells. The resulting tissue is still flexible but possesses great tensile strength (extensibility about 4%, maximum load about 6000 N/cm^2). The tendon is surrounded by synovial sheaths, which help to prevent friction as the tendon moves. The function of the tendon is to transmit the forces generated by the gastrocnemius and soleus to the calcaneus, where it inserts at the midpoint along the back surface of the bone (65-66). Achilles tendon also plays a role in energy storage and release during the performance of articular movements (67).

Plantar fascia (or plantar aponeurosis) is a wide, dense ligament of the sole of the foot – much denser than the ligaments on the dorsum – which originates from the medial and lateral processes of the tuberosity of the calcaneus, covers the muscles of the sole and inserts at the level of the metatarsal heads. Together with connective tissue, it is bound to the skin of the sole. Its main role is to sustain the longitudinal arch of the foot during propulsion, and to absorb the forces exerted on the talus upon heel-strike and during the transfer of the load from rearfoot to forefoot (66,68).

When the foot is in contact with the ground, GRF acts under the calcaneus, the metatarsal heads and the toes. The resulting moments (around the medio-lateral axis of the foot) tend to flatten the longitudinal arch. Then, resistant horizontal forces occur inside the plantar fascia, and active forces originate in the intrinsic foot muscles to maintain the arch. During standing still, however, muscle activity is negligible, and the passive ligamentous structures of the sole of the foot undertake the stress of holding the bones together, with little muscular help (66).

Metatarso-phalangeal joints are hinge-like joints which play an essential role during the push-off phase of gait, when the forefoot and the toes are in contact with the ground and bear the body weight. A moment of dorsal flexion is produced at each joint under the action of GRF, which is resisted by the contraction of the toe flexors.

Hicks (69) well described a resulting “gripping action”, due to the concurrent contraction of the above muscles and the setting of a mechanism - which he called Windlass mechanism - aimed at locking the midtarsal bones and stabilising the arch (68-71). The distinction between active and passive contributions was first described by Mann and Inmann (72), and has been recently proposed again by Hamel (73). Morton, instead, sustained that the main support to the longitudinal arch is provided only by the ligaments and the skeletal structure (74).

The biomechanical consequence of the Windlass mechanism was thoroughly described by Perry (75), who identified three main steps of the mechanism: the inversion of the rearfoot, the pronation of the forefoot, and the locking of the midtarsal joints to form a high and stable longitudinal arch. She agreed that Achilles tendon and plantar fascia are the tendinous and ligamentous structures primarily involved in the process of stiffening the foot, thus rendering it a propulsive rigid lever.

From an experimental point of view, several authors have demonstrated the role of Achilles tendon and plantar fascia in the biomechanics of the foot (61, 76-78); measured the effects of

Achilles tendon lengthening (62-64) and plantar fascia rupture or release (79-83); proved the anatomical link of Achilles tendon, plantar fascia and metatarso-phalangeal joints by measuring the strain in the plantar fascia under various loading conditions of the Achilles tendon and under different angular positions of the metatarso-phalangeal joints (59-60).

Most of these studies were conducted *in vitro*. In the present study, instead, the thickness of Achilles tendon and of plantar fascia was measured *in vivo*, by using a commercial ultrasound device (84). Their functionality was then assessed in terms of foot-floor interaction under the metatarsal heads, by means of the above cited piezo-dynamometric platform, and by static measurements of passive angular excursion of the first metatarso-phalangeal joint. The ultimate aim was to speculate about the functionality of the described biomechanical unit (Achilles tendon plus plantar fascia plus metatarso-phalangeal joints) in the presence of diabetic neuropathy, and find relationships between functional alterations and increased peak pressures under the metatarsal heads.

Tools and models for the clinical screening of patients at risk of ulceration

Peak pressure curve

Plantar pressure distribution is usually acquired during the preliminary screening of diabetic patients. Once the measurement protocol is standardised, and the accuracy of the measurement equipment verified, the elaboration of plantar pressure distribution in terms of ground reaction force and pattern of center of pressure may deliver useful information about the potential immediate risk of ulceration. However, in this part of the study attention was paid to the accurate analysis of another meaningful parameter, the Peak Pressure Curve (PPC), obtained by linearly interpolating the successive maximum values of pressure during the whole stance phase of gait. PPCs of controls and diabetic patients, with or without peripheral neuropathy and previous ulcers, have been analysed, in order to identify the effects of Limited Joint Mobility (LJM) of the foot-ankle complex, Muscular Weakness (MW) of plantar and dorsal flexors, and Increased plantar Peak Pressures (IPP). More specifically, a K-means algorithm (85) was applied to investigate the possibility of distinguishing the above effects on the basis of significant changes in the shape and amplitude of PPC.

Relationship between clinical and biomechanical variables

The present study confirmed that, from a biomechanical point of view, peripheral neuropathy results in significant alterations of gait, in terms of foot-floor interaction, but also at the level of the ankle articular complex, in terms of limited joint mobility and reduced muscular strength.

This last part of the study aimed at using multiple regressive models to associate the alterations of the biomechanical parameters measured at the ankle complex with concurrent alterations of physical and clinical parameters of diabetic patients, with or without neuropathy, namely height, body weight, body mass index, Vibratory Perception Threshold (VPT) and age. VPT is expressed in Volt, and is the most suitable clinical variable that accounts for severity of sensory neuropathy.

EXPERIMENTAL DESIGN

Functional analysis *vs* foot modelling

Even though various biomechanical models have been developed so far to study the properties and behaviour of the foot (86), the present study focuses on the design of instrumentation and methodologies for the functional assessment of the foot-ankle complex and for the definition of a functional model of the diabetic neuropathic foot. The rationale for the choice of experimentally assessing the residual function of such pathologic foot mainly originates from the multiple, and partially unknown, changes that diabetes and diabetic neuropathy induce in both foot-ankle structure and function. Under these conditions, some of the assumptions which are mandatory for the application of the current models might become wrong. Furthermore, some constant values used in the models might significantly change, and their direct measurement on the patients was not applicable within the research project described in the present study. Diabetes, and diabetic neuropathy, in fact, entail progressive changes in material characterisation of bones, cartilage, connective tissues, ligaments, muscles, joints, soft plantar tissues, which can be hardly taken into account when using even complex foot model simulations (77, 82, 87-88). On the other hand, the above changes may significantly alter the function of the foot-ankle complex, especially when they occur together with poor circulation and serious deformities of the anatomical foot structure.

Thus, a deeper knowledge of the functional impairments and residual ability of diabetic foot is mandatory, and the need is felt for an accurate quantification of main biomechanical parameters of gait and foot-floor interaction.

The experimental, functional assessment approach might also be of great help in the design of innovative models, i.e. computational models based on finite element methods, leading to new predictions, both in terms of an inverse analysis (explanation of mechanisms which lead to a given state) and a forward analysis (prediction of outcome of an intervention). Computational models, in fact, include characterisation of problem geometry and topology, boundary conditions, characterisation of material behaviour (relation between stresses and strains expressed through constitutive laws), nonlinear interface and contact conditions, and, most important, the evolution of material properties (inelasticity and damage) and components function, as it occurs with the progress of the disease.

Overview of the experimental design

For the purposes of the present study, a measurement laboratory for gait analysis was purposely designed and set up, using the basic equipment available at the Laboratory of Biomedical Engineering of the ISS. From a technical point of view, this activity mainly dealt with hardware and software integration and synchronization of commercial instrumentation, and design, calibration, validation and management of dedicated measurement devices. The laboratory was set up at the Department of Internal Medicine of the University “Tor Vergata” (Rome, Italy), where the clinical investigation was designed and conducted.

The first part of the laboratory investigation dealt with the assessment of the main kinetic parameters of foot-floor interaction. More specifically, three specific foot subareas were identified, namely heel, metatarsals, and hallux. For each of them, and for the total foot, the

following parameters were measured or estimated: local instantaneous components of GRF, istantaneous maximum pressures, COP trajectories. Data were acquired by two commercial dynamometric platforms (Bertec Corp., USA), one dedicated piezo-resistive pressure platform (27) and one commercial piezo-capacitive pressure platform (EMED ST-4, Novel Gmbh, Germany). Pressure platforms were rigidly fixed onto the dynamometric platforms, and signals from all four devices were synchronised. Patients were examined while walking barefoot and without any constraint. Trials with clear alterations of typical walking patterns were discarded before applying data averaging techniques.

For each of the functional blocks under study the following specific measurements were performed:

i) Assessment of the maximum angular excursions of the ankle articular complex in the sagittal, transversal and frontal anatomical reference planes. Excursions were measured by means of an ankle measurement device designed and constructed at the Laboratory of Biomedical Engineering of the ISS. With the patient seated and his/her leg and foot fixed to the device, every movement can be blocked alternatively in one or more reference planes; the patient is then able to perform active movements without experiencing significant load (at the beginning of the exercise, with the foot in a neutral position, the device is correctly balanced; during the movement the patient only experiences the inertia due to the device and the foot). The assessment of the angular excursion of the first metatarso-phalangeal joint (MPJ) was done manually, under passive applied torque. The patient was lying prone, with the knee flexed at 90° and the foot in neutral position with respect to the shank. The mechanical goniometer was centred on the examined joint, and all measurements were performed by the same operator.

ii) Assessment of the muscular functionality of the main plantar and dorsal flexors of the ankle articular complex. Measurements with respect to the three anatomical reference planes were collected with the same ankle measurement device. The device is also sensorized in order to measure the amplitude of the torques exerted around axes parallel to the axes of its three, mutually orthogonal, shafts. The device is equipped with three independent blocking systems which allow the ankle complex to be analysed in any desired angular position. In this case the patient was seated with knee flexed at 90°, his tibia inclined 20° with respect to the horizontal plane and parallel to the first member of the device; his foot was initially at 90° (with respect to the tibia) in the sagittal plane and 0° in the transversal and frontal planes. The patient was asked to perform isometric maximal contractions to produce torques around each axis, in both directions. Torques around the medio-lateral axis were further investigated by repeating the same exercise with the foot at 15° and 30° plantar flexion and 15° dorsal flexion.

iii) Assessment of the thickening of tendinous and ligamentous structures of the foot and ankle complex. Ultrasound measurements were done to check the absence of any significant alteration of the anatomic structure due to concurrent pathologies or previous traumas. Then measurements were obtained of the thickness of the main soft tissues, with special attention to Achilles tendon and plantar fascia, in both the frontal and sagittal planes. The patient was lying prone, with his leg flexed; the structures of interest were examined while the patient experienced a light tension. The measurement device was a commercial, high-resolution ultrasound device (Toshiba tosbee SSA 240, 8-10 MHz), and all the measurements were made by the same radiologist.

Detailed descriptions of each measurement phase, in terms of patients' identification, instrumentation, protocols and data management, are reported in the following paragraphs.

Recruited population

Sixty-one subjects from an outpatient clinic were recruited for the study: 27 diabetics without neuropathy (D) and 34 diabetics with neuropathy, 19 of whom without previous ulceration (DN) and 15 with previous ulceration (DPU). Twenty one age-matched healthy volunteers were recruited to serve as control group (C); the anamnesis and an objective clinical examination excluded neuro-musculo-skeletal pathologies in all the volunteers that may influence their gait.

The study was approved by the local ethics committee and all the subjects gave their written informed consent before the screening, in accordance with the principles of the Helsinki Declaration.

The inclusion criterion for diabetic patients was diagnosis of diabetes mellitus type 1 or 2 under stable metabolic control. The exclusion criteria were, for all subjects: age over 65 years; significant neurological diseases (except for those related to diabetic neuropathy); muscular/orthopaedic problems; inability to ambulate independently without pain; use of a walking aid; evidence of peripheral vascular disease (ankle brachial pressure index <0.85 and symptoms of intermittent claudication). The neuropathic patients were also excluded if they had active foot ulcers, previous minor or major amputations or Charcot's joints.

The clinical history evaluation included sex, age, height and weight to calculate the Body Mass Index (BMI), history of smoking and, for diabetic patients, duration of the disease, metabolic control (HbA1c) and presence of other chronic complications (retinopathy and nephropathy).

The presence of diabetic peripheral neuropathy was confirmed when the Neuropathy Disability Score (NDS) was greater than 5/10 and the vibration perception threshold (VPT, measured in Volt) at the hallux greater than 25 V (89). All patients in diabetic group D (without neuropathy) had NDS ≤4 and VPT <25 V. VPT was assessed by using a commercial Biothesiometer (Horwell, Nottingham, UK) on the tip of great toe. The mean value was calculated over three readings.

The NDS (25,90) is the product of scoring ankle reflexes (0 = normal; 1 = present on reinforcement; 2 = absent), plus vibration, pin-prick, and temperature sensation (cold tuning fork) at the hallux (0 = normal; 1 = abnormal). The maximum NDS (left and right legs combined) is 10, and scores of 3-5, 6-8, 9-10 were defined as evidence of mild, moderate and severe signs of neuropathy, respectively.

The DPU group included patients with a previous neuropathic ulcer healed for at least three months. All the previous ulcerations were localized at the metatarsal heads.

If present, callosities were removed before measurements.

Articular ultrasound examination was requested for both diabetic patients and controls.

Foot-floor interaction

Measurement systems

The present paragraph deals with the description of the innovative device (Figure 1) and the mathematical model used to evaluate the main biomechanical parameters of the foot-floor interaction (27). A "piezo-dynamometric" platform was obtained by rigidly fixing a dedicated pressure platform – designed and constructed at the Laboratory of Biomedical Engineering of the ISS – onto a commercial force platform (Bertec Corp., Worthington, OH, USA), in order to allow the resultant GRF to be transmitted unaltered from one platform to the other. The pressure

platform is made of a matrix of resistive sensors spaced 5 mm in both directions. Its acquisition rate can be set up to 100 Hz.

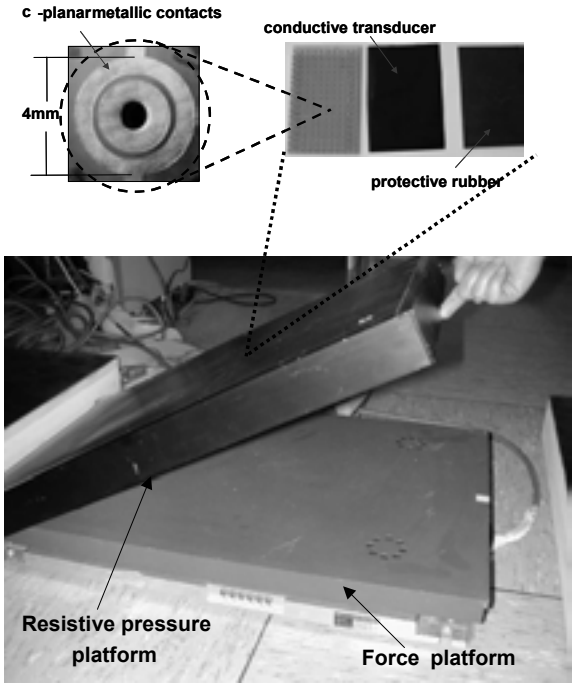

Figure 1. Piezo-dynamometric platform obtained by the superimposition of a dedicated pressure platform onto a commercial force platform (Bertec Co., USA): detailed view of the sensor technology used for the piezo-resistive sensor matrix

The force platform has a resolution of 2 N for force components and 0.3 Nm for moment components. Its resonance frequencies, 250 Hz for the horizontal modes and 500 Hz for the vertical mode, are only slightly diminished to 236 Hz and 472 Hz, respectively, because of the additional 2.4 kg mass of the pressure platform.

The resulting compound instrument simultaneously measures, for each sample, the GRF resultant (vertical and tangential components, free moment and location of the COP), and pressure distribution throughout the foot-to-floor contact area. The measurement of the vertical local GRF components delivered by the pressure platform, together with the measurement of the global GRF components measured by the force platform, allows for the computation of the local tangential forces acting on elementary areas. Thus, each foot subarea of interest, of any shape and dimension, can be completely characterised from a dynamic point of view.

Local vertical forces, acting on the surface covered by a single pressure sensor, are measured during each sampling, and an instantaneously changing coefficient k_i is calculated as the ratio between the instantaneous local vertical force f_{zi} and the instantaneous global vertical value F_z. To estimate the instantaneous local tangential GRF components f_{xi} and f_{yi}, the coefficient is then multiplied by the anterior-posterior (F_x) and the medio-lateral (F_y) instantaneous global value, respectively. The local tangential force f_{Mi}, generated by the free moment M that acts about a vertical axis passing through the COP of the total foot, further contributes to the above tangential components. This estimation is based on the hypothesis that there is a sample-by-

sample changing proportionality between the local vertical and tangential forces. The hypothesis comes from the observation that a foot loaded to half of the body weight can generate half the tangential force of a foot with 100% body weight. This hypothesis has been frequently formulated in the literature: i) Scott & Winter (43) made this assumption to calculate the moments at seven joints of the foot, as from the measurements of the vertical reactions of the seven related areas and the total tangential forces; ii) Abuzzahab *et al.* (91-92) made the same assumption when calculating the kinematic and kinetic data necessary to solve an inverse dynamics problem related to a four-segment model of leg, ankle and foot; iii) the moment patterns and ranges they found were in good agreement with similar quantities reported by Gage (93). To estimate the tangential GRF components (F_{xA}, F_{yA}) acting on a subarea A, we applied the following relationships which, as explained in (27), are valid under simplifying assumptions:

$$F_{xA} = \sum_A A_{ki} F_x - \sum_A A \left| f_{Mi} \right| \sin \alpha_i \, x \qquad [1]$$

$$F_{yA} = \sum_A A_{ki} F_y + \sum_A A \left| f_{Mi} \right| \cos \alpha_i \, y \qquad [2]$$

where x and y are the unit vectors of the x-axis and y-axis, respectively.

Their meaning can be better understood by making reference to Figure 2.

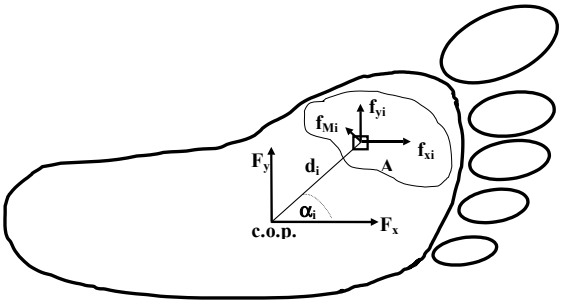

Figure 2. Tangential forces acting on an elementary area; f_{xi} and f_{yi} contribute to the global tangential forces F_x and F_y, respectively; f_{Mi} contributes to the moment that acts about a vertical axis passing through the COP of the total foot. "A" is a hypothetical foot subarea of interest

The results were qualitatively comparable with those reported by Akhlaghi and Pepper (94), who developed the Kent shear system – a portable system constituted by discrete tangential transducers – and reported the longitudinal and the transverse responses of 4 transducers placed under the big toe, the first and the fifth metatarsal heads, and the heel.

While measuring COP, the great advantage of using this compound instrument rather than a pressure platform or a force platform alone, mainly consists in its enhanced accuracy. In fact, the coefficient calculated to correct the absolute force value delivered by the pressure platform on the basis of the corresponding value delivered by the force platform improves the accuracy of the pressure data (27). And once the pressure platform is calibrated, it estimates COP more accurately than the force platform, in which the error depends on the position of the foot and increases as the foot approaches the borders of the platform. COP is here computed according to its definition, i.e., as the mean value of the sensors coordinates, weighted by the local pressure level.

A conceptually similar device was obtained by superimposing the commercial piezo-capacitive pressure platform (EMED ST-4, Novel, Germany) onto the second commercial force platform.

The capacitive pressure platform, 2 cm thick, 17 kg mass, pressure range 1-127 N/cm^2, has a smaller sensitive area (19 x 36 cm^2) than the resistive one (40 x 60 cm^2), same spatial resolution (4 sensors/cm^2), and lower sampling rate (50 instead of 100 Hz). Even though the platform is quite heavy, once rigidly fixed to the other it does not interfere too much with the force platform, whose resonance frequencies further decrease to 184 Hz for GRF horizontal components and to 368 Hz for vertical components.

The EMED system, based on capacitive sensors, does not suffer from hysteresis and creep, thus allowing correct measurements of plantar pressure distribution even under static conditions. For this reason it was included in the measurement equipment. In fact, static measurements have been also acquired, for each patient, even though the interpretation of the related data is out of the scope of the present study and will be not discussed in this context. However, the device has few drawbacks which suggested the simultaneous use of the two piezo-dynamometric systems instead of replacing the previous one. First of all, its small sensitive surface hardly contains a complete footprint, unless the patient is forced to centre it or a great amount of steps are acquired for each patient. Secondly, it is a commercial, close system, with its own hardware and software acquisition tools. Its synchronisation with the underlying platform was obtained on the basis of the first contact between foot and ground, but the implementation of the algorithm for the estimation of the local shear GRF components would have been taken too long, well beyond the time schedule of the present study.

Experimental set up and measurement protocol

The two integrated platforms were inserted at a level in the middle of a wooden walkway 6.4 m long, 0.8 m wide and 0.09 m thick. The length of the walkway allowed the patient to perform at least three steps before reaching the resistive piezo-dynamometric system (system 1), and at least two steps after the capacitive piezo-dynamometric system (system 2); this guaranteed that the acquisitions were made “at regimen” (95-96). Both the walkway and the platform of system 1 were covered with the same 3 mm-black protective rubber in order to avoid any influence on the patient’s gait. Platform of system 2 was already covered with a similar black rubber. The patient was trained to walk barefoot on the walkway at his preferred speed in a natural way, and to centre the active surface of system 1 with one foot only, without looking down at the platform. He was assured that centring or not system 2 had none relevance at all. At the end of the training phase, six complete footprints were acquired for each foot from system 1, and a range from 0 to 6 complete footprints were collected from system 2. Biomechanical data were stored together with the other relevant anthropometric and general data of the patient. The elaboration procedures described below only refers to data from system 1. Even though the platforms work independently of the direction of progression, the sample was always acquired with the patient walking in the same direction, in order to avoid artifacts due to visual asymmetries of the environment. For each foot of each patient three specific subareas were selected: the hallux, the metatarsals and the heel (Figure 3). Manual selection was recognized to be accurate enough for the selected subareas, and independent of the alteration of the geometric characteristics of the footprint. The operators were trained to select the end of the heel and the beginning of the metatarsals by making reference to the lines at 40% and 70% of the total length perpendicular to the bisecting line of the foot. The repeatability of this selection criterion was tested by means of the standard ANalysis Of VAriance (ANOVA) conducted on a critical footprint, where the heel was connected to the metatarsals through a wide midfoot region. The

ANOVA for multiple experiments was performed on force values resulting from four selections of each subarea per operator, and for four different operators. F values revealed that intra-operator differences were always not significant. As regards inter-operator differences, mean values and standard deviations of each operator's averaged values were analysed (SD was expressed as coefficient of variation – i.e. percentage of the mean values): all operators identified the hallux in the same way; SD was never beyond 1.5% for the heel; SD for the metatarsals was up to 1.5% for force ranges and up to 5% for force integrals.

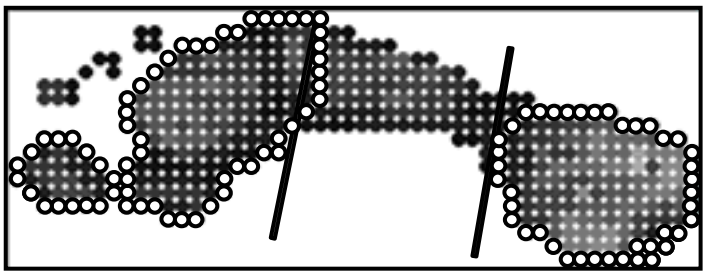

Figure 3. Pressure footprint - obtained from integrated system 1 - based on the local maximum pressure levels recorded during the whole stance phase of gait (the brightest the sensor, the highest the pressure). Three subareas are defined (white circles): heel, metatarsals, and hallux

For the sake of accuracy, all the selections used in this study were performed by the same operator.

As regards COP, the correct averaging and comparison of its trajectories called for minimisation of errors due to the great variability of stance phase duration, ab-adduction angle and foot size. To overcome these problems, the footprints were re-aligned and normalized with respect to the foot length and width, and the temporal curves resampled with respect to 256 samples and linearly interpolated. The spatial re-alignment basically consisted in the rotation and translation of the reference system solid with the footprint in order to make it coincide with the reference system of the platform. In order to define the former reference system, the bisecting line, which represents the anterior-posterior axis of the foot, was previously identified on the footprint. According to the guidelines delivered in the CAMARC II European Project (97), it was defined as the line which splits into equal parts the angle between the inner and the external tangents to the footprint. The medio-lateral axis of the foot-based reference system was then defined as the line perperdicular to the bisecting line and passing through the most distal point of the calcaneus.

Finally, in order to compare COP trajectories of different patients, curve length and width were normalised with respect to footprint length and width. Integrals were normalised with respect to the area of the rectangular box which contained the footprint. The left-foot COP curves were 180° rotated around the longitudinal axis in order to compare them with the right-foot curves.

Statistical analysis

For each foot of each patient, the data related to each trial for the total foot and the three selected subareas were normalized with respect to the body weight (b.w.), and temporally resampled in order to be averaged. Mean values and standard deviations were evaluated over six

trials for each foot. Each patient's feet were studied separately because of the physiological differences between them. Thus two contributions were obtained from every patient except those in the DPU class, for whom only the previously ulcerated foot was included in the study.

The one-way ANOVA was performed on the raw data of each class to obtain comparisons between multiple groups (one independent factor; four levels; four independent groups; $p<0.05$). For post hoc multiple comparisons of the means, Bonferroni test was used for equal variance.

Among the analysed biomechanical parameters, this study focused on the peak values and the ranges of the forces, expressed as a percentage of body weight (% b.w.). As for COP data, its trajectories under the total foot, and loading times of the total foot and the three selected subareas were analysed in this study.

Joint mobility and muscular functionality of the foot-ankle complex

This paragraph deals with the detailed description of a novel measurement system purposely designed and constructed for the *in vivo* characterisation of the ankle articular complex.

Mechanical description of the ankle measurement device

The mechanical system was designed to detect foot displacements with respect to the shank, and torques at the ankle articular complex. It basically consists of an open loop, seven links, and a six-DOF chain. The device and a detailed sketch of it are reported in Figure 4 and Figure 5 respectively.

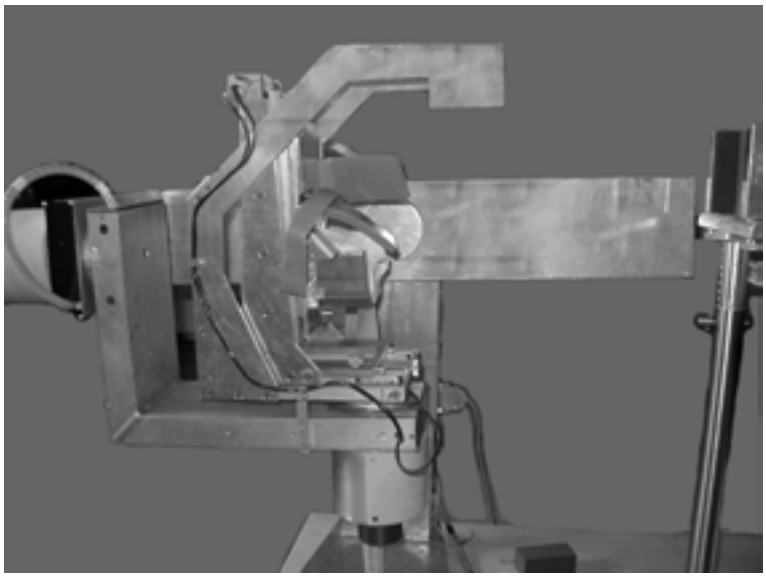

Figure 5. Ankle measurement device

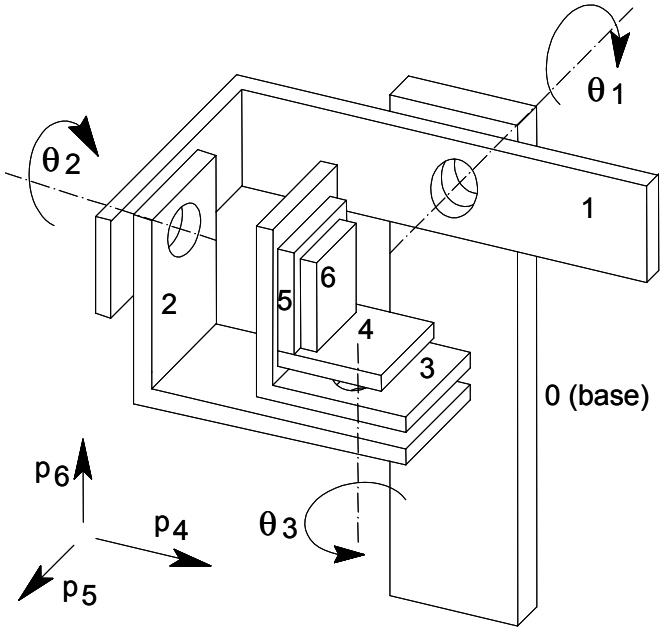

Figure 6. Sketch of the 7 link- 6 DOF mechanical chain (link 0 is solid with the patient's shank, link 6 with his/her foot)

The 7 links are connected through three revolute joints for angular movements, and three prismatic joints for linear movements. Measurements of torques are possible in any desired fixed position, by blocking the revolute joints by means of an electro-magnetic system. Angular movements are measured by three angular potentiometers solid with the revolute joints; linear movements, by three linear potentiometers solid with the prismatic joints.

The patient is seated on a three-DOF adjustable seat and his/her foot is positioned and fixed to plate 6. Forefoot is blocked by velcro stripes. Undesirable relative movements between rearfoot and plate are prevented by means of an aluminium block for the calcaneus, with the interposition of a polymethylsiloxane mould, prepared on a single subject's calcaneus so that to accurately reproduce even small details of its surface. Extended or flexed, the leg – at the level of the knee – is tied to a fork-shaped support rigidly fixed to the base link.

The mechanical layout has been so designed as to render the axes of the device as close as possible to the middle point of the segment connecting the tips of the medial and lateral malleoli. The axes of the anatomical reference system solid with the shank and with the base link result from the mutual intersections of the sagittal, transversal and frontal planes. The 3 axes of the foot reference system, which is solid with the device final link (link 6), coincide with the anterior-posterior axis of the foot (axis of inversion/eversion), with the line connecting the tips of the medial and lateral malleoli (axis of dorsal/plantar flexion) and with the line perpendicular to plate 6 (axis of internal/external rotation) (98). With the transformation matrix T, computed over Denavit-Hartenberg notation (99), position and orientation of the foot (reference system solid with the end link) are then related with respect to the shank (reference system solid with the frame link). A detailed description of the applied methodology and related computations is reported in (100). Briefly, it is just worth to note here that two main assumptions have been made: i) small constructive errors in the alignment of the device links

were considered negligible; ii) in the initial configuration, fixed and mobile reference systems were assumed to coincide. Denavit-Hartenberg parameters were accurately determined by using optical methods with direct reading precision of 0.01° (WILD Theodolite T2mod, WILD HEERBRUGG, Switzerland).

A further transformation is then mandatory to determine the kinematics of the foot frame in the Cartesian space, since the matrix T relates the joint variables vector to the displacements and rotations of the foot. The Jacobian matrix of the mechanism (matrix J), which maps the six-dimensional joint rate vector into the six-dimensional vector of Cartesian velocities, is then calculated. Thanks to the duality of kinematics and statics, the transpose of the same matrix J relates joint torques to generalised force exerted over link 6.

Electronic features of the device

Torques are measured through 3 extensometric bridges (Measurement Group, Inc., Raleigh, North Carolina, USA), so mounted as to transduce the torsional strain of the shafts of the 3 revolute joints. Bridge excitation was established at 5 V as a trade-off between power consumption and sensitivity. Sensitivity was further enhanced by using a full-bridge configuration, which also guarantees for minimal offset thermal drift. The transducers have been positioned as far as possible from the discontinuities of the shaft section, in order to avoid measuring border effects. Connecting cables have been properly soft-solded in order not to transmit potential cable tension to the strain gage. The output signal was amplified and filtered before being sampled and acquired through a commercial A/D converter (DAQ-Card, National Instruments). Minimum amplifier gains were adjusted to obtain torque ranges according to the literature (101), which suggested ±250 Nm for flexion-extension, and ±20 Nm for both inversion-eversion and internal-external rotation. To improve resolution at lower torques, two further gain values can be set for each amplifier, when needed. Amplified signals were finally low-pass filtered at 10 Hz.

The joint rotation angles are measured by means of angular precision potentiometers (Series 357-0-0-502 by Spectrol, input voltage 10 V) with elements in conductive plastic and bushing mount format. Translations are measured with linear potentiometers (Leane International, Parma, input voltage 10 V).

The potentiometers outputs are connected to voltage-followers to have low impedance voltage signals. Each signal from the voltage-followers was properly amplified in order to measure, in correspondence with maximum ouput range (±5 V): ±100° in dorsi-plantar flexion, ±50° in internal-external rotation and ±50° in prono-supination. Offsets were regulated in order to set zero-voltage signals in correspondence with the initial reference position of the ankle joints (90° between foot and shank in the sagittal plane, 0° in the other two planes; knee flexed at 90°, shank rotated at 20° backwards with respect to the perpendicular to the ground). Signals were low-pass filtered at 10 Hz.

Moments or torque transducers were accurately calibrated by applying known moments at each axis on which they are surmounted. For each transducer calibration a proper configurations of the mechanical chain was used to theoretically nullify the moments due to gravity, therefore calibrating moments were composed of one known component given by a dynamometer (IMADA, range 0-1000 N, resolution 1 N) applied at known lever arm. Sensitivity was then assessed for each torque at each possible amplifier gain. Final calibration tests confirmed that high linearity was achieved in the desired torque range (minimum gain: slope = 0.016, R^2 = 0.997; medium gain: slope = 0.046, R^2 = 0.999; maximum gain: slope = 0.099, R^2 = 0.993). Sensitivity was found in the range 0.02-0.71 V/Nm. Predicted sensitivity was verified for both

angular (flexion-extension: 0.05 V/°; internal-external rotation: 0.1 V/°; prono-supination: 0.1 V/°) and linear (0.2 V/mm) potentiometers.

The 9 voltage signals are acquired by means of the A/D converter ATMIO-64F5 (National Instruments, resolution 12 bits, input range +10 V) at 1024 Hz. This specific board was chosen because of its capacity to acquire up to 64 single-ended analog signals. Thus the ankle measurement device can be used in conjunction with other measurement devices, such as multi-channels EMG amplifiers.

Experimental configuration

The ankle measurement device was synchronised with a commercial surface EMG amplifier (ASE16 by LISIN, Turin, Italy) which uses peculiar electrode arrays where myoelectric signals are simultaneously captured by 16 unipolar or 15 differential, equally spaced electric contacts. Besides computing the usual temporal and spectral parameters of EMG signal, this device yields a good estimation of the velocity of conduction. Inter-electrode distances and array configurations can be chosen according to specific measurement needs.

In the described experimental set up, 7 differential EMG signals were simultaneously captured along each of two investigated muscles, namely the tibialis anterior and the gastrocnemius; thus 2 electrode arrays were used, 8 contacts each, with 10 mm inter-electrode distance.

The rationale behind this choice was the monitoring of the muscle activity before each contraction. The acquired data will also supply useful information about time and level of muscle activation under different isometric configurations; however, the study of myoelectrical activity is beyond the scope of the present study, and the interpretation of the related data will be not discussed in the following.

The patient's right shank was aligned to the first link of the mechanical chain, previously rotated of +20° with respect to the horizontal plane. In this way the knee was 90°-flexed, and the subject could sit in a more comfortable position. His foot was blocked at 90° with respect to the shank in the sagittal plane, and at 0° in the other two planes (frontal and transversal). This specific configuration (neutral position) guarantees for the measured torques to be directly referred to the anatomical reference system. Patient was first trained to perform the correct isometric contraction starting from resting condition. In this phase the visual feedback of the EMG software was proved to be very helpful. Patient was then asked to perform a sequence of isometric maximal contractions to produce torques/moments around each axis, in each direction. Each contraction lasted 10 s, and was followed by 90 s of rest. Moments around the medio-lateral axis were further investigated by repeating the same exercise with the foot at 15° and 30° of plantar flexion and 15° of dorsal flexion, respectively Figure 6). Maximum values were corrected with respect to the initial offset, and then normalised with respect to BMI. This normalisation was chosen in the attempt to take into account not only the dependence of muscle length and moment arm on the height of the patient, but also their eventual dependence on the mass of the bony structure. An ideal BMI of 30 was then introduced in order to espress torques/moments as "normalised" Nm.

As regards angular excursions, maximal excursions in the directions of flexion-extension, internal-external rotation and inversion-eversion were acquired while the patient was performing slow cycles for a total duration of 10s. Absolute maximum angular value in each direction was then identified and included in the study.

The metatarsal joint motion was manually assessed by means of a general-purpose, long-arm mechanical goniometer. The total range of motion at the 1st metatarso-phalangeal joint was measured as follows: with the patient lying prone and with the subtalar joint in neutral position,

the maximal flexion and extension ranges of the hallux were then determined with the goniometer centred in the examined joint, its long arm aligned to the medial side of the heel and its short arm aligned to the hallux. For the sake of accuracy, the range of motion was recorded for both feet of each patient by the same operator.

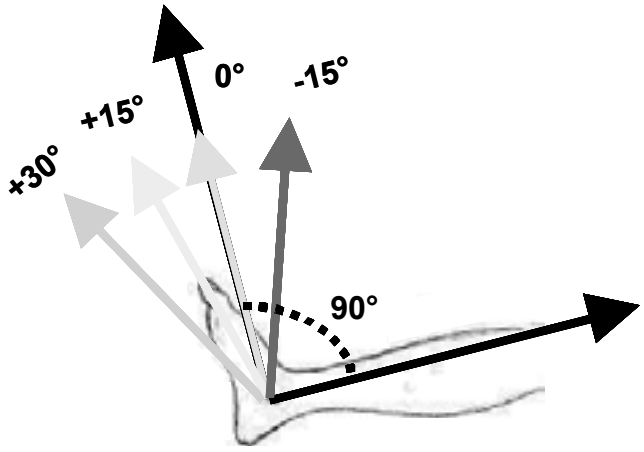

Figure 6. Sagittal view of the foot-ankle complex. Isometric contractions were performed with the foot at 0° of internal/external rotation, 0° of inversion/eversion, and 0° of flexion/extension (neutral position). Flexion/extension moment was also performed at 15° of dorsal flexion, and 15° and 30° of plantar flexion

Statistical analysis

Basic non parametric statistics (Mann-Whitney U test, $p<0.05$) was used to find potential significant alterations of both muscular and articular measured parameters.

Functionality of tendinous and ligamentous structures of the foot-ankle complex

The ultrasound examination of articular surfaces and soft tissues was made by using a high-resolution, 8-10 MHz linear array (Toshiba tosbee SSA 240). All exams were performed by a rheumatologist experienced in musculo-skeletal ultrasound technique. Thickness of tendinous and ligamentous structures of the foot-ankle complex was examined in both feet. Thickness of Achilles tendon and plantar fascia was measured under slight tension, with the patient lying prone, his leg 90° flexed with respect to the body, and the foot in neutral position. Measurements were taken in the frontal and sagittal planes, and expressed in mm. Thickness was observed for the whole length of the two soft structures, but measurements were taken in correspondence with their insertion on the calcaneus. Pathologic thickness was defined with respect to reference values of 4 mm (±0.5 mm) for Achilles tendon and 2 mm (±0.5 mm) for plantar fascia.

Statistical analysis

Non parametric statistics (Spearman, $p<0.05$; Mann-Whitney U test, $p<0.05$) were used to highlight correlations among Achilles tendon thickness, plantar fascia thickness, peak vertical forces under the metatarsals, and 1st metatarso-phalangeal joint mobility, and to show significant alterations of each of the above parameters among the examined groups of patients and controls.

Tools and models for the clinical screening of patients at risk of ulceration

Peak pressure curve

Peak Pressure Curves (PPC) were obtained, for this specific part of the study, from the EMED ST-4 capacitive pressure platform. High reliability of the data was guaranteed by the fact that they were acquired while the patients did not worry about hitting the platform, by the high number of complete footprints acquired notwithstanding the "don't care" advise, and by the high accuracy and very low noise of the capacitive pressure sensors. Only one more healthy volunteer was included in this part of the study with respect to the previously described population, for whom only the force data were corrupted. Thus 22 healthy volunteers were included in the study as control group, matched for age and physical characteristics with the diabetic patients. The pathologic group was formed by 50 out of the 61 diabetic patients – those who had hit the EMED platform at least three times per foot – ; as with controls, the two lower limbs were considered separately for each patient. An ad hoc clinical classification, based on the Vibratory Perception Threshold (VPT) and Neuropathy Disability Score (NDS), was made in this specific study, aimed at separating those patients with "mild" neuropathy from those with almost absent signs of neuropathy. Patients were thus classified as "pure diabetics" (D) if NDS was lower or equal to 2 and VPT was lower or equal to 10 V; "severe neuropathic diabetics" (S) if NDS was greater or equal to 6 and VPT was greater or equal to 25 V, and "diabetics with mild neuropathy" (M) in any other case.

Data for the assessment of ankle LJM and MW were extracted from the bulk of data acquired with the described ankle measurement device. Peak values were identified for each and every patient and healthy volunteer. 25° and 75° percentiles were then calculated for the control group and used to define ranges of normality.

PPCs were normalized to 100% of the stance phase, resampled over 256 samples, and averaged over three curves for each foot of each patient/healthy volunteer. Resampled PPCs were averaged over 42 curves inside the control group, and 25°, 50° and 75° percentiles were used to define a range of normality.

Ninety seven pathologic PPCs, obtained from diabetic patients with or without neuropathy, were grouped according to the single or simultaneous LJM, MW and IPP assessed for each leg of each patient. The latter parameter was calculated with respect to the reference maximum peak pressure value (plus one standard deviation). More specifically, the curves were included in group A if associated with IPP, LJM and MW; included in group B if associated with LJM and MW only; included in group C if associated with IPP only; included in group D if not associated with any significant motor impairment; discarded if referred to previously ulcerated, contra-lateral feet and/or associated with other pathologies (group E). This sub-division was defined as *functional classification*.

A second sub-division of patients, defined as *shape-based classification*, was done on the basis of the shape and amplitude of PPCs. A K-means clustering algorithm (three clusters, stop at 10 iterations, random initial centroids) was implemented and applied to the 97 patients' PPCs (85). Mean curve, median curve, 25° and 75° percentiles were calculated for each cluster. Mean curves were then compared with those of groups A and B. Mean values and standard deviations were calculated, inside each cluster, for each parameter of interest, and basic statistical techniques were applied. More specifically, one-way ANOVA (1 independent factor; 4 levels; 4 independent groups) was performed for the 3 clusters and for the control group, and multiple comparisons, with Bonferroni correction, were performed with respect to controls ($p<0.05$).

Relationship between clinical and biomechanical variables

The control group consisted of 21 healthy volunteers (9 females, 13 males) matched for age and physical characteristics with the diabetic patients. The pathologic group was formed by 60 diabetics, 26 females and 34 males, whose VPT (vibratory perception threshold) was measured according to the existing guidelines (90) and included in the study as the only clinical variable of the model.

Table 1 shows mean values and standard deviations of the chosen independent variables. Student's t-test confirmed that there were no statistically significant differences between the two groups (controls and patients) for any of the variables but for BMI ($p=0.05$).

Table 1. Mean values and standard deviations of independent variables of patients and controls which have been included in the regressive model

Group	Cases	Age (yr)	Height (cm)	Weight (kg)	BMI (kg/m^2)	VPT (V)
Controls	22	50.41 (±14.6)	168.55 (±8.8)	71.00 (±11.3)	24.86 (±2.6)	-
Diabetics	60	53.97 (±12.8)	168.20 (±9.7)	76.42 (±15.6)	26.97 (±4.8)	13.00 (±8.3)

As for the biomechanical variables, namely ankle joint mobility and torques due to muscular isometric contractions, their assessment has already been described earlier in this section.

For the control group, a set of statistical regressive models have been considered whose independent variables were sex, age, height, body weight and BMI. The best fitting model was then applied to the pathologic group, too, with the inclusion of the clinical variable VPT among the independent factors of the model.

RESULTS

A general overview is reported in the following which deals the most relevant results obtained from the whole functional assessment of the post-ankle complex in patients and controls. As for the baseline patient characteristics, there were no significant differences between groups for age, BMI, metabolic control or diabetes duration. VPT and NDS were significantly increased in DN with respect to D and C; in DPU they were significantly increased also with respect to DN (Table 2).

Table 2. Baseline patient characteristics

Characteristic		C	D	DN	DPU
Number		21	27	19	15
M / F		13 / 8	19 / 8	10 / 9	10 / 5
Age (years)	*mean*	56.6	52.7	53.7	57.3
	SD	11.8	12.7	10.4	9.6
BMI (kg /cm²)	*mean*	25.0	25.3	27.0	27.5
	SD	3.1	3.4	4.9	4.1
Type 1 / Type 2		-	8 / 19	9 / 10	3 / 12
Diabetes duration (years)	*mean*	-	15.1	19.4	16.9
	SD	-	9.3	9.3	8.6
HbA1c (%)	*mean*	-	7.5	7.8	7.3
	SD	-	1.5	1.8	2.4
VPT toe (V)	*mean*	5.3	14.7	31.5 ∗	39.9 ∗†
	SD	2.1	5.7	7.6	13.3
NDS	*mean*	0	3.8	6.95 ∗	7.9 ∗†
	range	-	0-5	6-8	7-9
Retinopathy (a / b / p)		-	24 / 0 / 3	9 / 5 / 5	5 / 3 / 7
Nephropathy (a / m / M)		-	26 / 1 / 0	16 / 2 / 1	15 / 0 / 0

C: control group; D: diabetic patients without neuropathy; DN: diabetic with neuropathy; DPU: diabetic patients with previous ulceration; (a / b / p = absent, background, proliferative; a / m / M = absent / microalbuminuria / macroalbuminuria)
*p<0.05 *vs* D; †p<0.05 *vs* DN

The assessment of the functionality of the ankle articular complex in diabetic patients, with and without peripheral neuropathy, showed a general trend towards the reduction of the range of motion in all planes of the anatomic reference system, and in both directions. The more severe the neuropathy, the greater the impairment, but, surprisingly enough, limitations were also evident in diabetic patients with NDS and/or VPT below the common neuropathic thresholds. Joint mobility impairment was greater in the sagittal plane than in the other two planes, and in dorsal flexion more than in plantar flexion. Statistical non parametric analysis (Mann-Whitney U test, $p<0.05$) highlighted the following significant differences with respect to C group: D patients showed significantly diminished dorsal flexion; DN patients showed LJM in the sagittal and in the transversal planes; DPU patients showed joint mobility reduction in all planes and all directions of movement.

A progressive reduction of joint mobility throughout the pathologic classes was also observed with respect to the 1st metatarso-phalangeal joint. Again, non parametric tests (Spearman test, $p<0.05$) confirmed the statistical significance of the reduction of the range of motion.

A similar decreasing trend was observed with respect to the muscular functionality of the foot-ankle complex. Also in this case a major reduction was measured in correspondence with moments due to the action of ankle dorsal flexors in the sagittal plane. Non parametric tests (Mann-Whitney U test, $p<0.05$) revealed the following significant differences: i) D patients significantly reduced moments during dorsal flexion (sagittal plane), apart from those produced with the foot blocked at 15° of dorsal flexion, and torques expressed in the transversal plane; ii) DN patients showed reduced moments in the sagittal plane (at each foot position with respect to dorsal flexion, at 30° of plantar flexion with respect to plantar flexion) and with respect to eversion (frontal plane), and reduced torques in the transversal plane. High variability was found in the distribution of torques expressed by DPU patients. Thus the statistical analysis only highlighted significant differences for torques related to external rotation (transversal plane), moments related to plantar and dorsal flexion (sagittal plane) with the foot at 30° of plantar flexion, moments related to dorsal flexion with the foot at 15° of plantar flexion.

Differences in the thickness of Achilles tendon and plantar fascia were also examined by using non parametric statistic tests (Spearman test, $p<0.05$), which showed that the increased thickness found for all pathologic classes and for both soft structures was statistically significant for all patients, with a greater increase in neuropathic patients.

The analysis of foot-floor interaction delivered useful information which were in total agreement with data reported in the specialised literature, together with further peculiar information about the alterations of the GRF horizontal components and of the COP pattern. Alterations with respect to reference force values were found in all pathologic classes, even though statistical significance was hardly demonstrated for D patients. Differences related to DN and DPU patients, instead, were nearly always proved to be statistically significant. More specifically, the study highlighted the following alterations of gait: loading times of the heel and of the metatarsal heads percentually increased with respect to the duration of the whole stance phase; load under the hallux was dramatically reduced; GRF anterior-posterior force showed lower peaks both at landing and during propulsion; GRF medio-lateral components increased in correspondence with the metatarsal heads during propulsion; COP pattern showed a shift of the load towards the longitudinal axis of the foot, with greater involvement of the central and medial structures of the foot.

The following are detailed reports of the elaborated data regarding each functional block and the analysis of foot-floor interaction. Data are also reported about the PPC shape-based classification and the regressive models fitting.

Foot-floor interaction

Table 3 reports mean values and standard deviations for the peaks of GRF vertical component.

Table 3. Peak value of vertical component of GRF (% b.w.): mean values; SD

Group		Total foot	Heel	Metatarsals	Big toe
C	*mean*	108.8	93.8	89.9	21.9
	SD	5.2	8.4	6.3	9.2
D	*mean*	106.8	91.3	93.9	17.1 *
	SD	5.3	9.0	6.7	7.7
DN	*mean*	107.4	87.3 *	96.0 *	14.0 *
	SD	5.7	8.4	7.0	6.2
DPU	*mean*	107.0	83.1 *†	97.5 *	10.7 *†
	SD	9.1	11.1	7.0	6.4

* $p<0.05$ *vs* C; † $p<0.05$ *vs* D

As an example of the averaged force curves obtained for each foot subarea, the mean temporal evolution of GRF vertical component under the hallux is reported in Figure 7 for all classes.

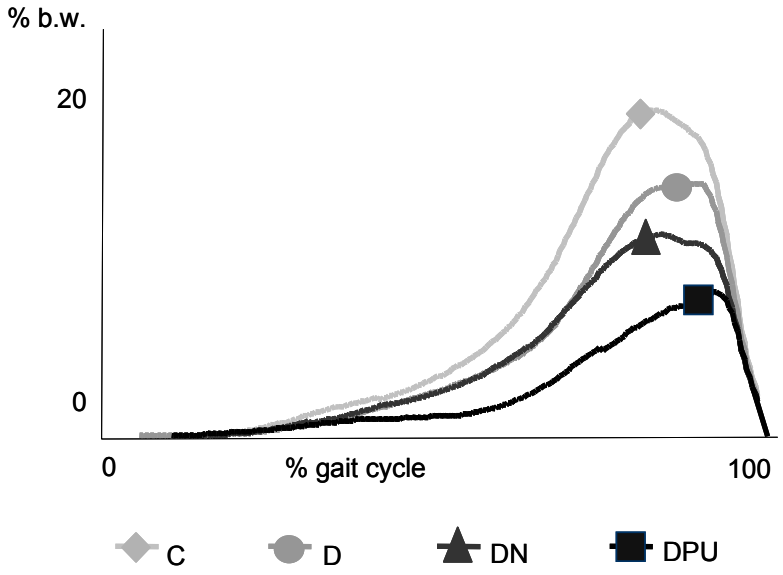

Figure 7. Averaged temporal evolution of the vertical GRF component under the hallux, for all classes of patients

The peak vertical force of the whole foot was similar in all groups. In the heel region the peak vertical force was significantly reduced in DPU *vs* D and C, and in DN *vs* C. In the metatarsal area, peak vertical forces were significantly higher in DN and DPU than in C. The hallux expressed a significantly reduced vertical force in DPU, DN and D *vs* C, and in DPU *vs* D.

The anterior-posterior component of GRF can be considered to be the sum of two main contributions: a forward curve, mainly recorded during the heel strike, and a backward curve mainly recorded during the push-off phase. In Table 4 the mean values and the standard deviations are reported for the peaks and the ranges of the anterior-posterior GRF component. The forward curves are reported in Figure 8 for the heel.

The peak force of the forward curve was significantly decreased for the total foot in DPU and DN *vs* C, and at the heel subarea in DPU and DN *vs* D and C. The peak force of the backward curve was significantly reduced in DPU and DN *vs* C for the total foot; it was similar in the four groups at the heel and in the metatarsal area, while in the hallux area a significant reduction was observed in DPU, DN and D *vs* C.

The medio-lateral component of GRF has a small component which represents the medial curve, and a greater component which represents the lateral curve, which is the most important part of this force.

In Table 5 the mean values and the standard deviations are reported for the peaks and the range of the medio-lateral GRF component.

The temporal evolution under the metatarsals is reported in Figure 10, where a significantly increased lateral peak is evident for DPU patients.

Table 4. Anterior-posterior component of GRF (% b.w.): mean values; SD

Group		Total foot	Heel	Metatarsals	Big toe
Forward peak					
C	*mean*	15.9	15.3	3.3	0.4
	SD	3.9	3.6	1.5	0.7
D	*mean*	15.2	14.8	2.6	0.5
	SD	3.3	3.4	1.4	0.6
DN	*mean*	13.3 *	12.5 *†	2.7	0.4
	SD	3.9	3.5	1.9	0.5
DPU	*mean*	13.3 *	11.8 *†	3.0	0.7
	SD	3.8	3.7	1.5	1.2
Backward peak					
C	*mean*	18.5	0.5	13.4	5.3
	SD	3.1	0.9	2.5	2.4
D	*mean*	16.6	0.4	13.2	3.8 *
	SD	3.7	0.8	3.3	2.0
DN	*mean*	15.3 *	0.9	12.6	3.1 *
	SD	3.7	1.3	3.2	1.9
DPU	*mean*	15.2 *	1.0	13.5	2.4 *
	SD	3.5	1.0	3.4	1.7
Range					
C	*mean*	34.4	15.8	16.6	5.7
	SD	6.3	3.5	3.1	2.2
D	*mean*	31.7	15.2	15.8	4.3 *
	SD	6.1	3.4	3.4	2.0
DN	*mean*	28.6 *	13.4 *	15.4	3.5 *
	SD	7.0	3.0	4.1	1.9
DPU	*mean*	28.5 *	12.8 *	16.6	3.1 *
	SD	7.4	4.1	4.4	1.8

* p<0.05 *vs* C; † p<0.05 *vs* D

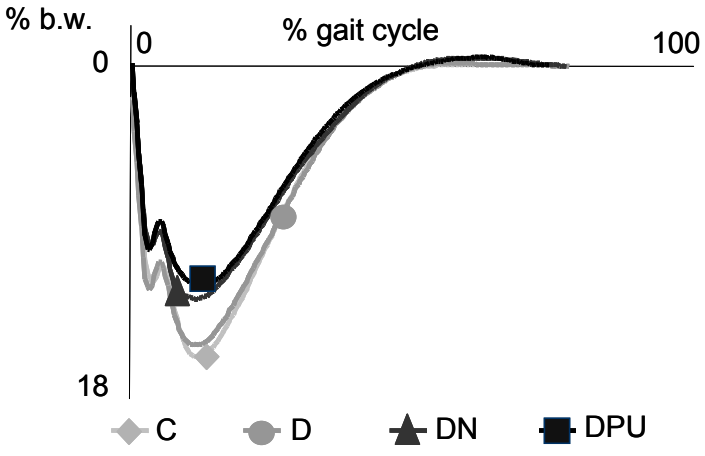

Figure 8. Averaged temporal evolution of the anterior-posterior GRF component under the heel, for all classes of patients

Table 5. Medio-lateral component of GRF (% b.w.): mean values; SD

Group		Total foot	Heel	Metatarsals	Big toe
Medial peak					
C	*mean*	4.4	4.4	0.5	0.8
	SD	2.4	2.4	0.6	0.7
D	*mean*	3.4	3.4	0.4	0.4 *
	SD	1.6	1.7	0.5	0.5
DN	*mean*	3.3	3.3	0.4	0.2 *
	SD	1.7	1.7	0.6	0.3
DPU	*mean*	3.9	3.9	0.4	0.3 *
	SD	1.8	1.8	0.7	0.4
Lateral peak					
C	*mean*	5.0	3.4	3.9	0.9
	SD	2.3	1.8	2.1	0.6
D	*mean*	5.0	3.5	4.3	0.7
	SD	2.2	1.9	2.0	0.5
DN	*mean*	5.2	3.6	4.4	0.7
	SD	2.3	1.7	2.1	0.5
DPU	*mean*	6.2	3.5	5.8 *	0.5 *
	SD	3.1	1.6	3.0	0.4
Range					
C	*mean*	9.4	7.7	4.5	1.7
	SD	2.7	2.4	1.8	0.7
D	*mean*	8.5	6.8	4.7	1.1 *
	SD	2.4	2.0	1.8	0.6
DN	*mean*	8.6	6.9	4.8	0.9 *
	SD	2.3	1.9	1.9	0.5
DPU	*mean*	10.1	7.4	6.2 *†	0.7 *
	SD	3.7	2.3	2.6	0.4

* p<0.05 *vs* C; † p<0.05 *vs* D

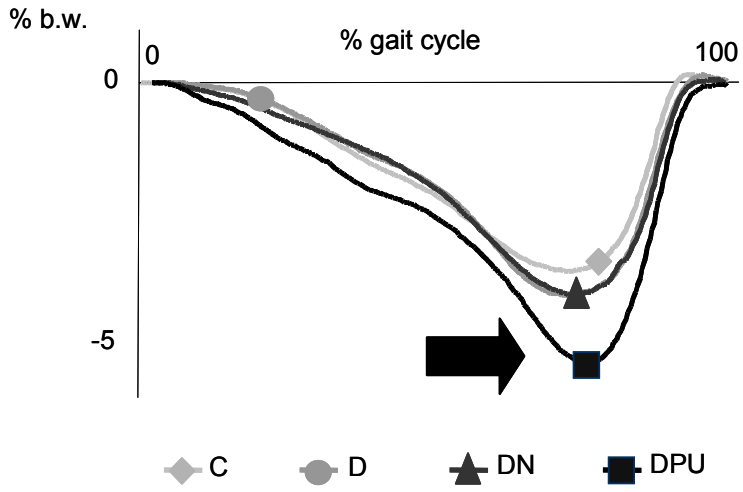

Figure 9. Averaged temporal evolution of the medio-lateral GRF component under the metatarsals, for all classes of patients

While no differences were recorded for peak values, ranges or integrals when considering the whole foot and the heel, in the metatarsal region the peak value of the lateral component was significantly higher in DPU than in C. Also the range values were significantly higher in DPU than in D and C. At the hallux level the force medial peak and range were significantly lower in DPU, DN and D *vs* C; the lateral peak and the integral were reduced in DPU *vs* C.

Several correlations were found between VPT and biomechanical parameters both for the whole foot and for the selected subareas, and are reported in Table 6.

Table 6. Correlation of biomechanical parameters with VPT

Parameters	Total foot	Heel	Metatarsals	Big toe
Vertical force / VPT				
Peak Value	-	r=0.36 p=0.0001	r=0.26 p=0.01	r=0.36 p=0.0001
Anterior-posterior force / VPT				
Forward Peak Value	r=0.28 p=0.0005	-	-	r=0.34 p=0.0001
Backward Peak Value	r=0.28 p=0.008	r=0.30 p=0.0002	-	-
Medio-lateral force / VPT				
Medial Peak Value	-	-	-	r=0.31 p=0.0001
Lateral Peak Value	r=0.20 p=0.02	-	r =0.24 p=0.003	-

As for the COP pattern, the averaged COP excursions were evaluated along both axes (longitudinal and medio-lateral) and the integral of the COP curve computed with respect to the longitudinal axis.

Figure 10 shows the averaged COP curve patterns from a qualitative point of view; it is worth noticing here the trend of the COP curve to reduce its excursion, with the raise of diabetes and with the increase of neuropathy, both medio-laterally and longitudinally.

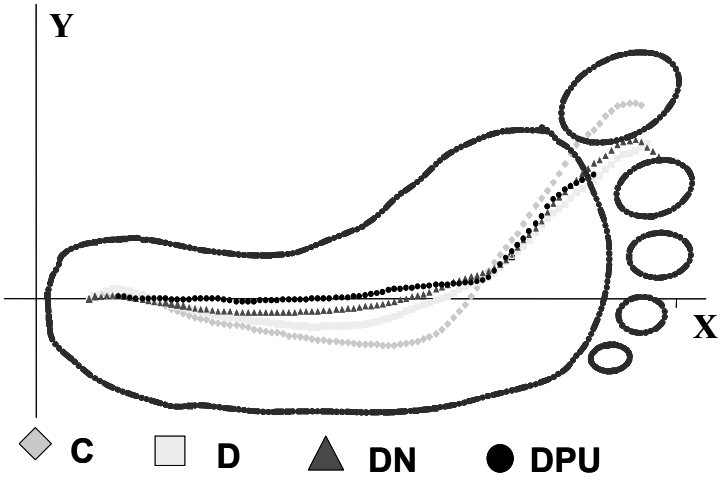

Figure 10. COP trajectories throughout the whole stance phase of gait, normalised with respect to a standardised footprint

In order to obtain quantitative information by a so effective parameter its excursion was computed along the longitudinal axis X and along the medio-lateral axis Y, and its integral under the curve (Figure 11).

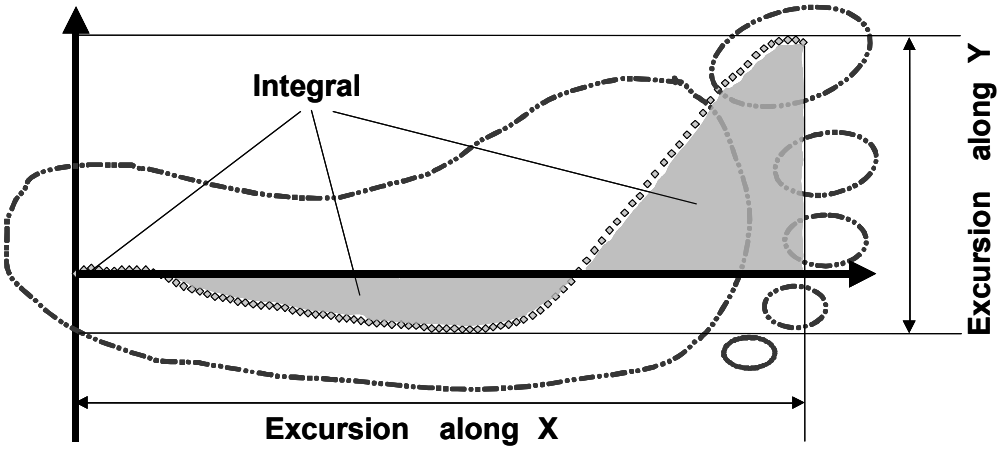

Figure 11. Definitions of COP parameters as quantified in the present study

Mean values of the maximum excursions along the longitudinal axis are reported in Figure 12. Only for DPU patients the differences with respect to controls were found to be statistically significant ($p < 0.05$).

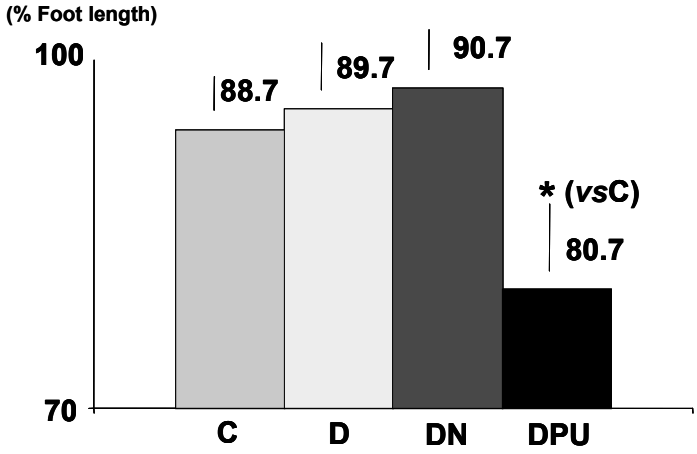

Figure 12. Maximum COP excursions along the longitudinal axis of the foot. '*' indicates statistical significance with respect to control group (Student's t-test, p<0.05).

Differences in the excursions along the medio-lateral axis (Figure 13) were instead clearly evident for all diabetic classes, even more evident for DPU patients.

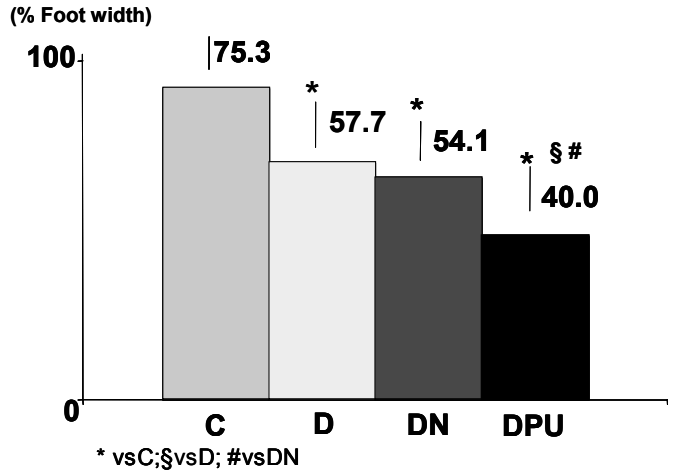

Figure 13. Maximum COP excursions along the medio-lateral axis of the foot. Statistical significance has been assessed by using one-way ANOVA (4 independent groups, p<0.05)

Finally, similar results were found for the integral of the COP curve related to the loading under the total foot (Figure 14).

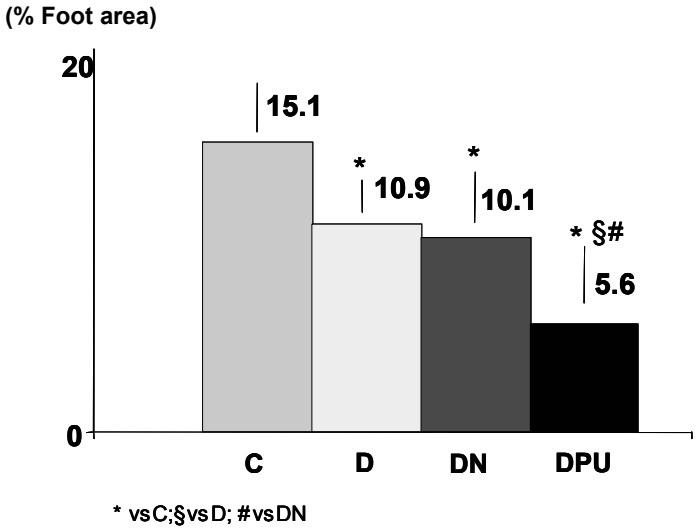

Figure 14. COP integrals (with respect to the longitudinal axis of the foot). Statistical significance has been assessed by using one-way ANOVA (4 independent groups, p<0.05)

COP excursions along the anterior-posterior and the medio-lateral axes of the footprint only account for eventual COP pattern alterations in the space domain, due to shifts of load under parts of the foot different from usual. No information about abnormal loading time could be extracted from such parameters. Thus a further analysis of the COP pattern that takes into account the temporal evolution of the curves throughout the whole phase of stance has been performed.

This COP pattern study in the time domain has helped in highlighting further critical modifications in the gait of diabetic patients, especially those without neuropathy. The most interesting results are summarised in Figure 15; for few subareas of interest, the hystograms show the time interval during which COP fell into the corresponding area. Special attention should be paid to the hystogram related to the metatarsals area (grey area), which clearly shows that COP remains for a very long time on the central metatarsals of diabetics, while it is definitely absent in correspondence with the hallux. In general, their trend is to shift the load towards the longitudinal axis of the foot, and this fact, surprisingly enough, should not be read as an effect of peripheral neuropathy but rather as a consequence of diabetes. As reported in Table 7, loading time was significantly longer in DN and DPU than in C group for total foot, heel and metatarsals; at the heel region it was significantly longer in DPU than in D. Hallux loading time for DPU was significantly shorter than in DN and D.

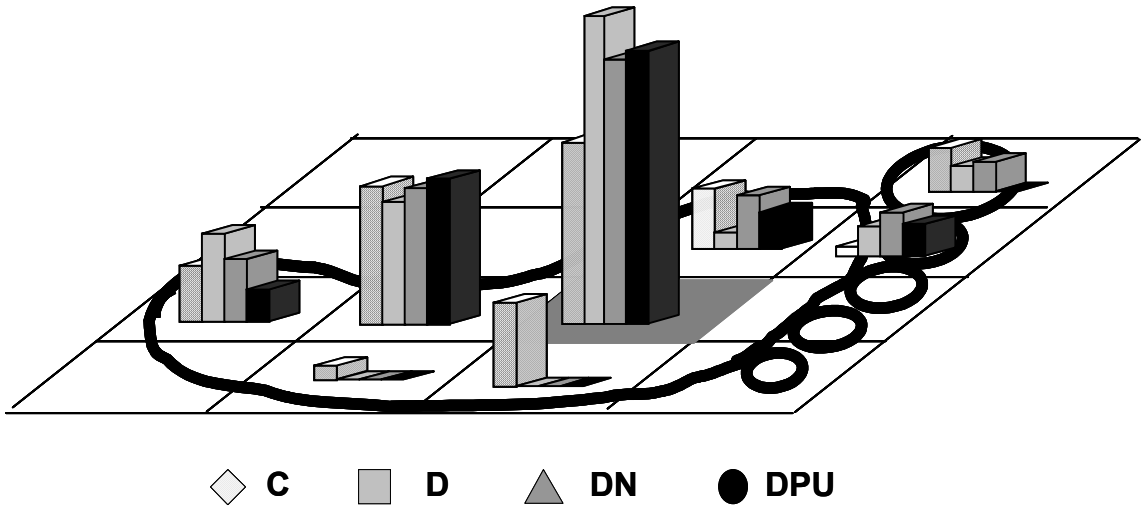

Figure 15. Histograms of COP instantaneous positions, under few specific foot subareas, throughout the whole phase of stance

Table 7. Mean value and standard deviation of foot loading time during gait, expressed in ms. Subarea loading time is also expressed as a percentage of the total foot loading

Group	Total foot	Heel	Metatarsals	Hallux
C	723.7 ± 65.7	427.1 ± 65.3 (59.0%)	638.2 ± 62.2 (88.2%)	446.4 ± 33.4 (61.6%)
D	766.5 ± 89.9	468.6 ± 91.3 (61.1%)	691.0 ± 75.8 (90.1%)	498.8 ± 43.2 (65.1%)
DN	828.6 ± 152.2 *	528.1 ± 133.9 (63.7%) *	759.8 ± 143.7 (91.7%) *	520.6 ± 86.4 (62.8%)
DPU	816.8 ± 150.6 *	547.7 ± 142.0 (67.1%) *†	760.5 ± 144.2 (93.0%) *	377.0 ± 98.5 (46.2%) †‡

* p<0.05 *vs* C; † p<0.05 *vs* D; ‡ p<0.05 *vs* DN

Joint mobility and muscular functionality of the foot-ankle complex

The evaluation of the joint mobility at the 1st metatarso-phalangeal joint showed a statistically significant reduction of the range of motion in all diabetic groups (Table 8).

Table 8. Joint mobility of the ankle articular complex in all reference planes and of the 1st metatarso-phalangeal joint in sagittal plane expressed in degrees (median values, 25° and 75° percentiles)

Reference plane	Degree	C	D	DN	DPU
Sagittal					
Dorsal flexion	*25° percentile*	28.7	24.5	22.8	23.4
	median	35.5	32.1*	26.7	26.9*
	75° percentile	38.7	35.2	32.2	31.2
Plantar flexion	*25° percentile*	33.3	33.0	28.2	29.6
	median	39.8	36.6	33.0	31.2*
	75° percentile	46.2	43.2	37.0	34.6
Range	*25° percentile*	62.4	58.7	52.3	56.0
	median	77.4	67.9	59.1	58.8*
	75° percentile	87.2	77.7	66.0	64.2
Transversal					
External rotation	*25° percentile*	36.7	26.9	27.6	28.2
	median	44.7	35.4	34.3*	31.9*
	75° percentile	47.9	47.5	41.9	42.0
Internal rotation	*25° percentile*	33.5	14.4	22.9	21.6
	median	38.8	34.3	26.1*	25.0*
	75° percentile	46.3	40.7	35.1	34.7
Range	*25° percentile*	73.4	41.3	50.9	50.1
	median	80.9	70.8	63.8*	60.6*
	75° percentile	92.6	87.8	76.1	74.7
Frontal					
Eversion	*25° percentile*	9.6	12.4	9.6	7.4
	median	13.9	16.7	11.7*	11.7*
	75° percentile	21.2	19.9	14.7	13.7
Inversion	*25° percentile*	26.9	24.0	26.6	21.7
	median	30.1	31.6	31.1	24.5*
	75° percentile	35.1	37.2	38.5	29.2
Range	*25° percentile*	40.9	35.2	37.6	33.0
	median	43.4	45.3	43.4*	37.4*
	75° percentile	51.1	55.4	51.5	41.5
Sagittal					
1st metatarso-phalangeal	*25° percentile*	93.1	42.7	46.8	37.3
joint	*median*	100.0	54.0*	54.9*	46.8*
	75° percentile	103.2	63.8	62.0	55.1

* (Mann-Whitney U test, $p<0.05$)

A general trend was observed towards the reduction of the range of motion in all planes and directions (Figures 16 and 17; Table 8), with surprising limitations also evident in diabetic patients with low NDS and VPT. Joint mobility impairment was greater in the sagittal plane than in the other two planes, and in dorsal flexion more than in plantar flexion. Statistical non

parametric analysis (Mann-Whitney U test, $p<0.05$) highlighted the following significant differences with respect to the control group: diabetic non neuropathic patients (D) showed significantly diminished dorsal flexion; diabetic neuropathic patients (DN) showed limited joint mobility in the sagittal and in the transversal planes; diabetic neuropathic patients with previous ulcers (DPU) showed joint mobility reduction in all planes and all directions of movement.

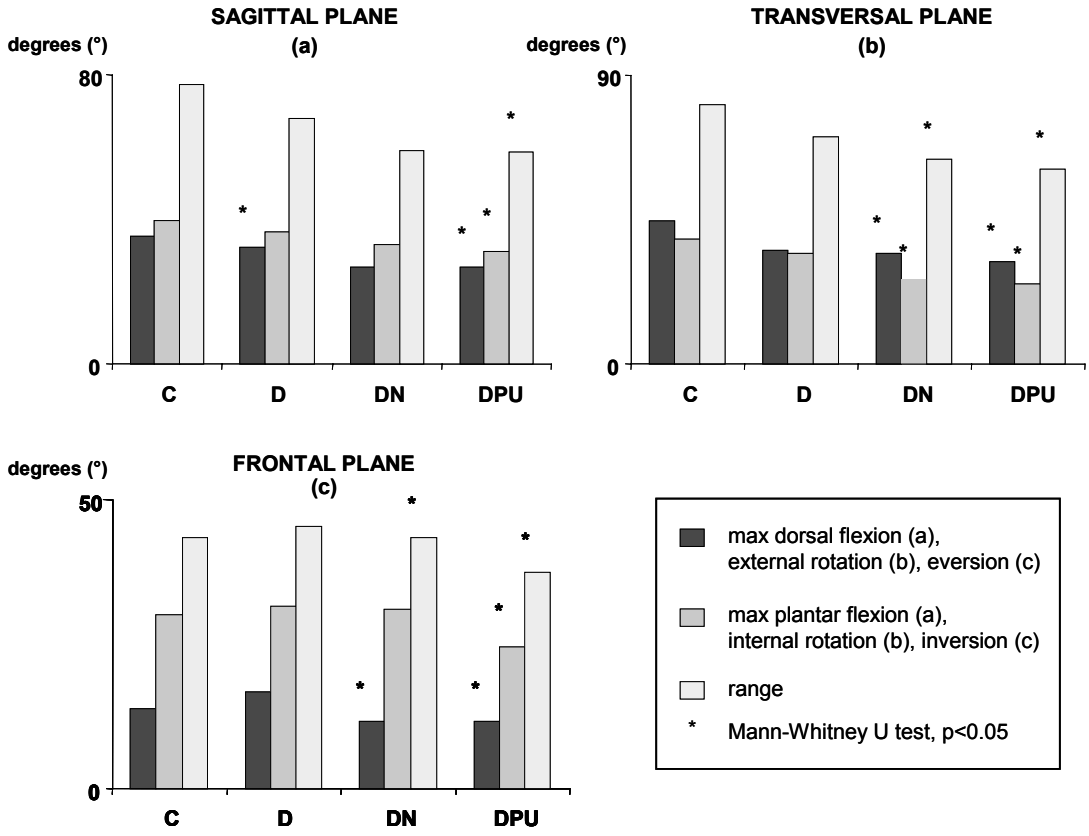

Figure 16. Joint mobility of the foot-ankle complex (median values)

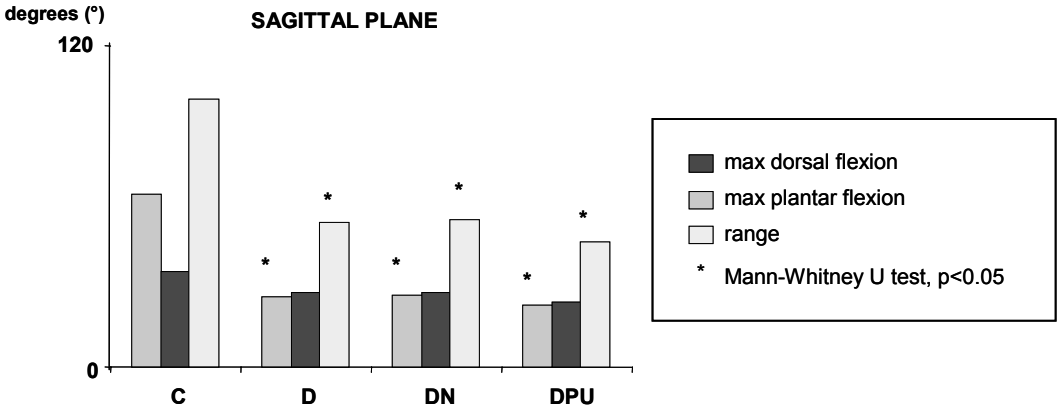

Figure 17. Joint mobility of the 1st metatarso-phalangeal joint in the sagittal plane (median values)

As for the muscular functionality of the foot-ankle complex, a major reduction was measured in correspondence with moments due to the action of ankle dorsal flexors in the sagittal plane (Figures 18 and 19; Table 9-10).

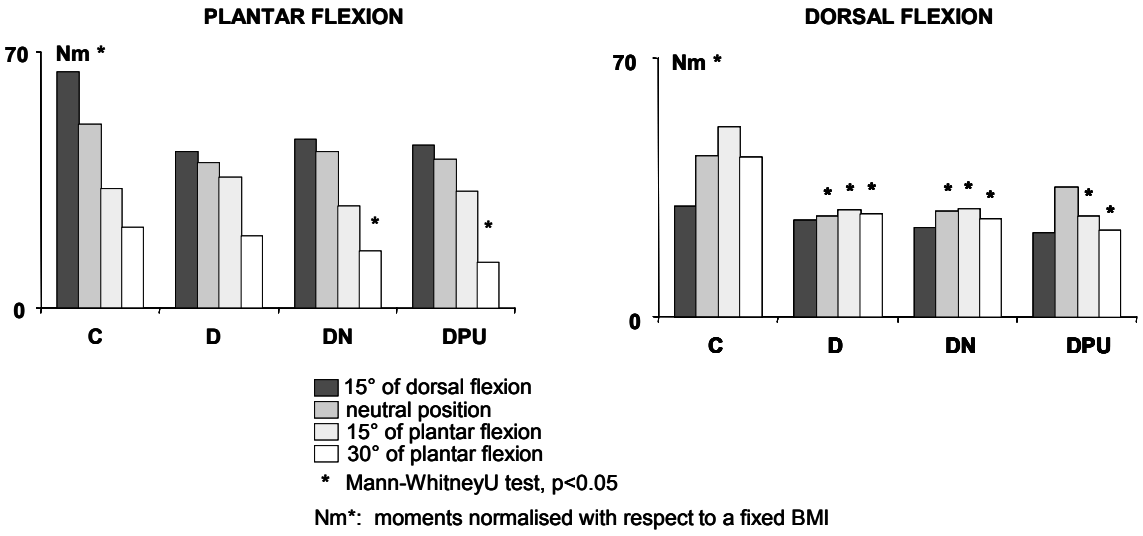

Figure 18. Moments of the foot-ankle complex around the medio-lateral axis (sagittal plane) (median values)

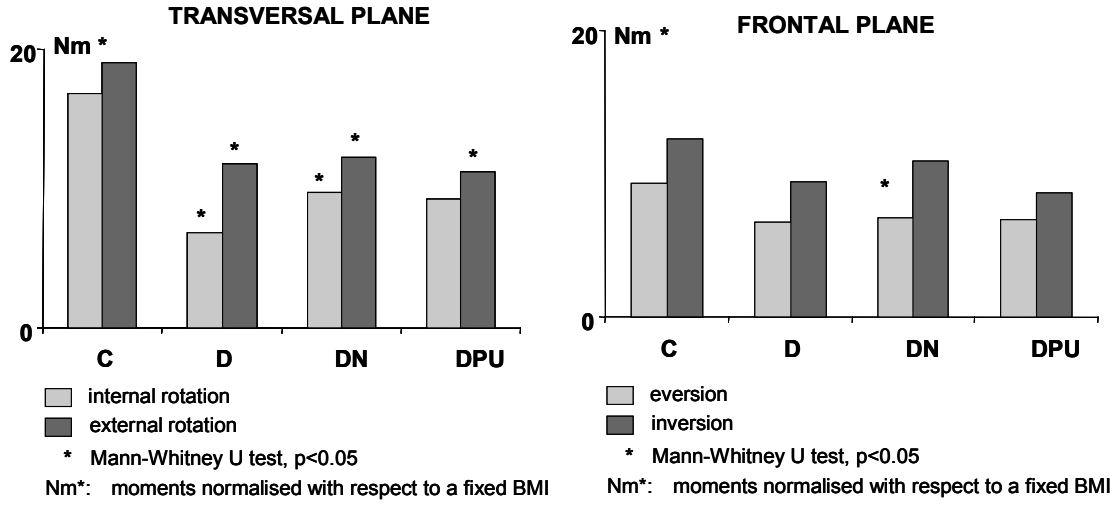

Figure 19. Foot ankle complex: torques around the vertical axis and inversion/eversion moments around the longitudinal axis (median values)

Table 9. Flexion (dorsal flexion) / extension (plantar flexion) moments at the ankle, normalised with respect to BMI (Nm*) (median values, 25° and 75° percentiles). Moments are referred to four angular positions in the sagittal plane: 15° of dorsal flexion (–15°); neutral position (0°); 15° and 30° of plantar flexion (+15°; +30°)

Measurement		C	D	DN	DPU
Plantar flexion					
at –15°	*25° percentile*	38.8	18.7	34.8	19.1
	median	64.5	42.7	46.2	44.4
	75° percentile	74.2	66.8	53.2	72.2
at 0°	*25° percentile*	34.7	19.3	32.8	22.1
	median	50.3	39.6	42.7	40.8
	75° percentile	68.6	52.8	55.7	69.5
at +15°	*25° percentile*	30.2	21.0	20.8	20.2
	median	32.8	35.7	28.0	32.0
	75° percentile	40.0	45.2	33.3	37.8
at +30°	*25° percentile*	10.0	10.8	8.6	10.1
	median	22.1	19.8	15.7*	12.5*
	75° percentile	27.9	25.9	20.1	14.9
Dorsal flexion					
at –15°	*25° percentile*	21.7	15.8	16.1	19.4
	median	30.0	26.0	24.3	22.7
	75° percentile	52.8	42.4	38.1	38.7
at 0°	*25° percentile*	32.3	13.4	21.3	23.7
	median	43.6	27.1*	28.5*	35.0
	75° percentile	63.9	46.7	45.4	59.2
at +15°	*25° percentile*	34.8	17.9	20.3	20.1
	median	51.2	28.7*	29.4*	27.1*
	75° percentile	59.1	50.6	40.4	52.6
at +30°	*25° percentile*	31.7	18.9	18.5	19.1
	median	43.2	27.7*	26.5*	23.5*
	75° percentile	49.1	35.1	34.1	36.1

* (Mann-Whitney U test, p<0.05)

Table 10. Internal/external torques and inversion/eversion moments at the ankle, normalised with respect to BMI (Nm*) (median values, 25° and 75° percentiles). Moments are referred to neutral position

Measurement		C	D	DN	DPU
Internal rotation	*25° percentile*	9.0	4.2	5.7	5.1
	median	16.8	6.8*	9.7*	9.2
	75° percentile	22.0	17.5	12.3	14.1
External rotation	*25° percentile*	13.0	8.1	7.7	7.9
	median	19.0	11.8*	12.2*	11.2*
	75° percentile	27.2	17.3	17.0	22.0
Inversion	*25° percentile*	7.7	5.7	5.6	5.4
	median	12.4	9.4	10.8	8.7
	75° percentile	17.2	12.5	14.4	12.6
Eversion	*25° percentile*	7.2	4.1	4.8	3.6
	median	9.3	6.6	6.9*	6.8
	75° percentile	13.2	9.5	9.0	12.1

* (Mann-Whitney U test, p<0.05)

Non parametric tests revealed the following significant differences: i) D patients significantly reduced moments during dorsal flexion (sagittal plane), apart from those produced with the foot blocked at 15° of dorsal flexion (Table 9), and torques expressed in the transversal plane (Table 10); ii) DN patients showed reduced moments in the sagittal plane (at each foot position with respect to dorsal flexion, at 30° of plantar flexion with respect to plantar flexion) (Table 9) and with respect to eversion (frontal plane), and reduced torques in the transversal plane (Table 10). High variability was found in the distribution of torques expressed by DPU patients. Thus the statistical analysis only highlighted significant differences for torques related to external rotation (transversal plane) (Table 10), moments related to plantar and dorsal flexion (sagittal plane) with the foot at 30° of plantar flexion, moments related to dorsal flexion with the foot at 15° of plantar flexion (Table 9).

Functionality of tendinous and ligamentous structures of the foot-ankle complex

Ultrasound examination showed a significant increase in plantar fascia thickness in all groups of patients in comparison with controls, as shown in Figure 20A) [D 2.9±1.2 mm, DN 3.0±0.8 mm, DPU 3.1±1.0 mm, C 2.0±0.5 mm ($p<0.05$)]. Thickness of Achilles tendon showed a similar trend, as reported in Figure 20B) [D 4.6±1.0 mm , DN 4.9±1.7 mm, DPU 5.2±1.7 mm, C 4.0±0.5 mm ($p<0.05$)]. A few results, already reported in the previous sections, have been repeated for they are part of the following correlations. The evaluation of the joint mobility at the 1st metatarso-phalangeal joint showed a reduction of the range of motion in all diabetic groups (Figure 20C).

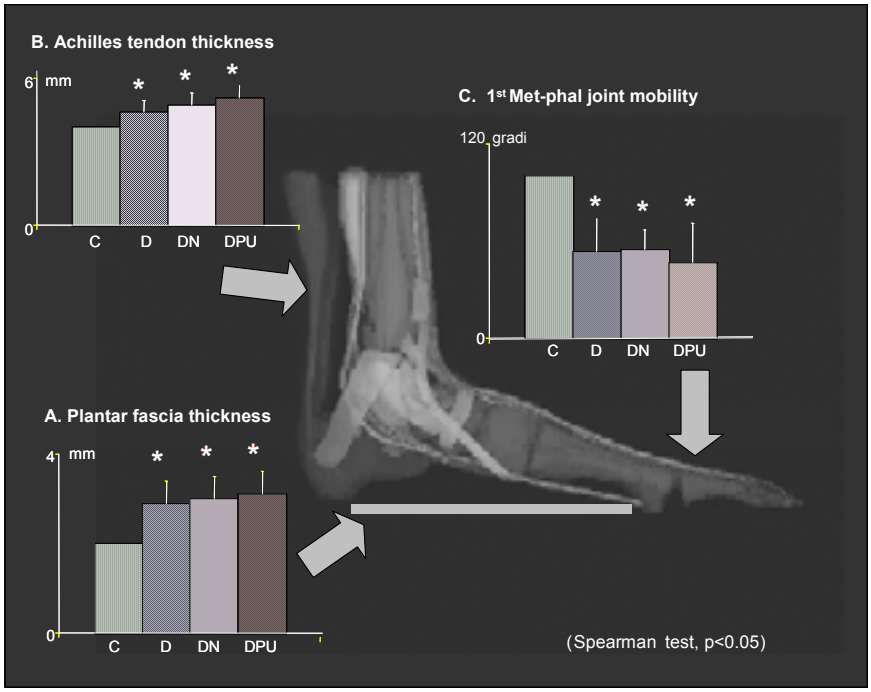

Figure 20. Median values of Achilles tendon thickness (expressed in mm), plantar fascia thickness (expressed in mm) and mobility of the 1st metatarso-phalangeal joint in the sagittal plane (expressed in degrees)

The study of foot-floor interaction under the metatarsals showed increased vertical forces in DN and DPU patients, and increased medio-lateral forces in the DPU group, as reported in Figure 21.

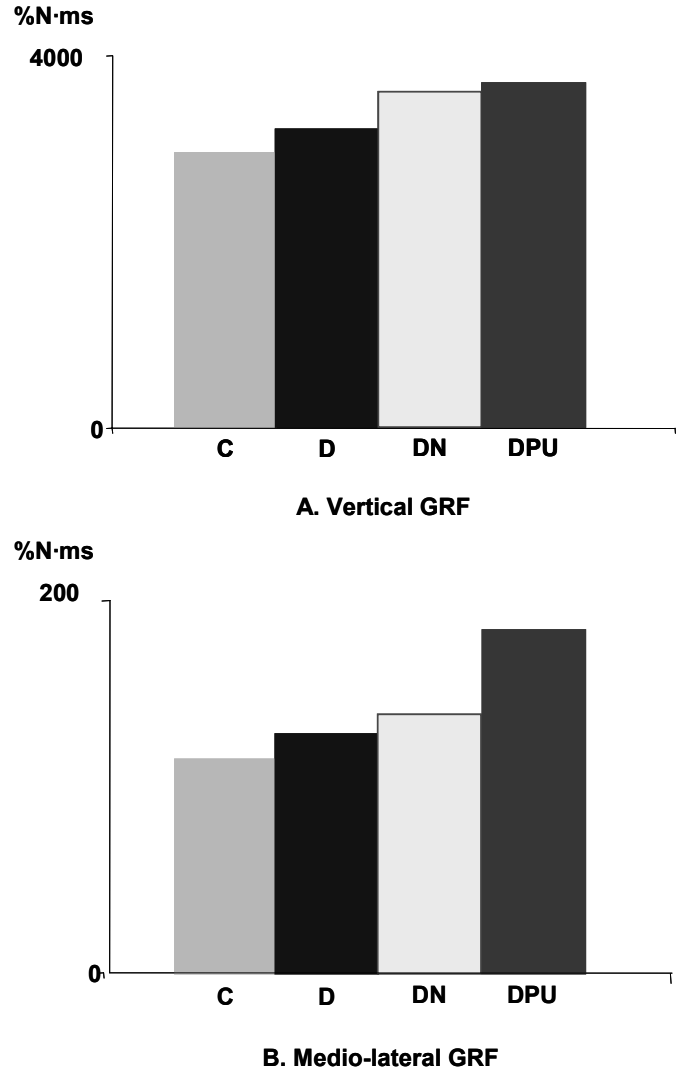

Figure 21. GRF under the metatarsal region: integrals of the vertical (A) and medio-lateral (B) components

Table 11 resumes: mean values and standard deviations of the integrals of the vertical, anterior-posterior and medio-lateral components of GRF, expressed as % of body weight (%N) times ms; mean values and standard deviations of Achilles Tendon Thickness (ATT), Plantar Fascia Thickness (PFT), and 1st Metatarso-Phalangeal angular Excursion (MPE). Among the GRF parameters, only Integral of the Vertical Forces under the Metatarsals (IVFM) is considered for regression analysis. Table 12 resumes the results of linear regressions for each couple of variables.

Table 11. Mean values and standard deviations of IVFM, integrals of vertical, anterior-posterior and medio-lateral components of GRF under the metatarsals, ATT, PFT and MPE

Parameter	Group			
	C	D	DN	DNPU
GRF				
vertical (%N·ms)(IVFM)	2956.8±430.5	3209.7 ±493.3	3625.2±695.3*°	3722.1±743.2*°
ant-posterior (%N·ms)	257.4±62.3	264.4±59.1	279.3±73.1	301.8±94.2
medio-lateral (%N·ms)	115.5±68.7	129.8±68.6	139.8±76.6	185.7±114.1*
ATT (mm)	4.0±0.5	4.6±1.0	4.9 ±1.7*°	5.2±1.7*°
PFT (mm)	2.0±0.5	2.9±1.2	3.0±0.8	3.1±1.0
MPE (°)	100.0±10.2	54.0±29.4	54.9±17.2	46.8±20.7*

(*p<0.05 *vs* C ° p<0.05 *vs* D)
ATT = Achilles Tendon Thickness; PFT = Plantar Fascia Thickness; MPE = 1st Metatarso-Phalangeal angular Excursion; IVFM = Integral of the Vertical Forces under the Metatarsals

Table 12. Correlations between each cuple of parameters ATT, PFT, MPE and IVFM

Correlation ($\|r\|>0.5$)	ATT	PFT	MPE	IVFM
ATT		*	*	
PFT	*		*	*
MPE	*	*		
IVFM		*		

(*p<0.05 *vs* C ° p<0.05 *vs* D)
ATT = Achilles Tendon Thickness; PFT = Plantar Fascia Thickness; MPE = 1st Metatarso-Phalangeal angular Excursion; IVFM = Integral of the Vertical Forces under the Metatarsals

An inverse correlation (r = -0.53) between PFT and MPE was found when considering the three pathologic groups altogether, as well as a direct correlation between PFT and IVFM (r = 0.52). No significant correlation was found between MPE. Figure 22 shows the regression line and equation for the relationship between PFT and MPE (A) and for the relationship between PFT and IMVF (B).

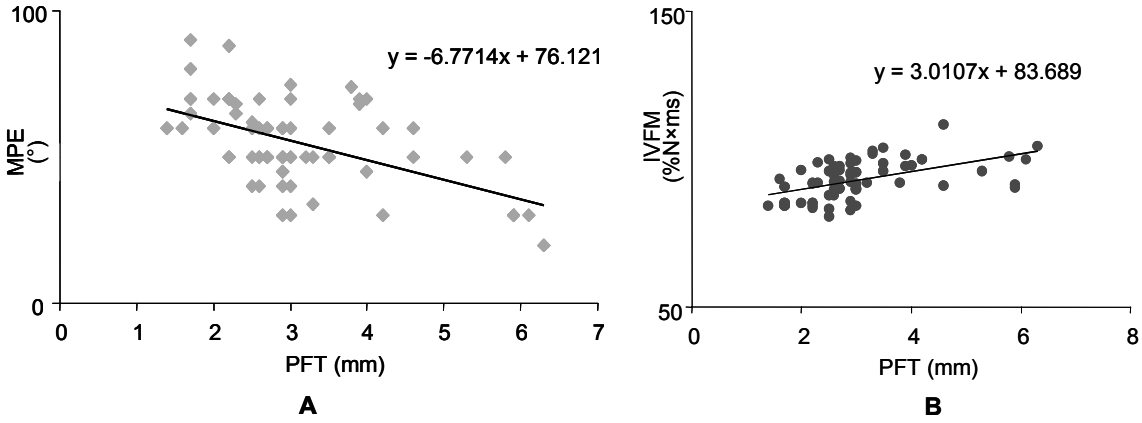

Figure 22. Regression line and equation for the relationship between PFT and MPE (A) and for the relationship between PFT and IVFM (B)

Notwithstanding the thickening of Achilles tendon and the concurrent increase of vertical GRF under the metatarsal heads, the correlation was not statistically significant. It was instead significant between thickening of Achilles tendon and impaired mobility of the 1st metatarso-phalangeal joint. As expected, the linear regression well fitted the relationship between the thickening of Achilles tendon and of plantar fascia (Table 11).

Tools and models for the clinical screening of patients at risk of ulceration

Peak pressure curve

Table 13 reports the clinical classification of the patients in diabetics with none (D), mild (M) or severe (S) neuropathy.

Table 13. Patients' neuropathy-based classification

Group	Criteria	Cases
D (diabetics)	(VPT<=10) and (NDS<=2)	25
M (mild)	(not D) or (not S)	45
S (severe)	(VPT>=25) and (NDS>=6)	27
Total		97

Figure 23 shows the reference values for PPC, calculated in correspondence with the 25° and 75° percentiles of the distribution of PPCs for 42 healthy cases.

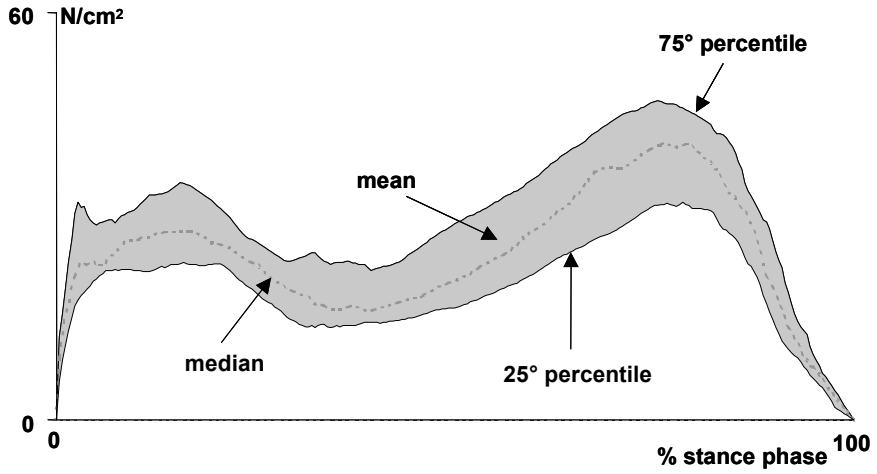

Figure 23. Reference temporal curves of PPC plotted for the whole stance phase of gait. The curves have been calculated in correspondence with the mean, the median, the 25° and the 75° percentile of the distribution of PPCs for 42 healthy cases

Figure 24 summarises the most important results of the functional and shape-based classification. Figure 24A) plots the mean curves obtained on the basis of the functional classification for group A (IPP+LJM+MW) and group B (LJM+MW). The application of the shape-based algorithm led to the definition of three, well-defined clusters, reported in Figure 28B). The shape of the corresponding curves seems to be strongly related to functional impairments of diabetic gait, as clearly shown in Figure 24C).

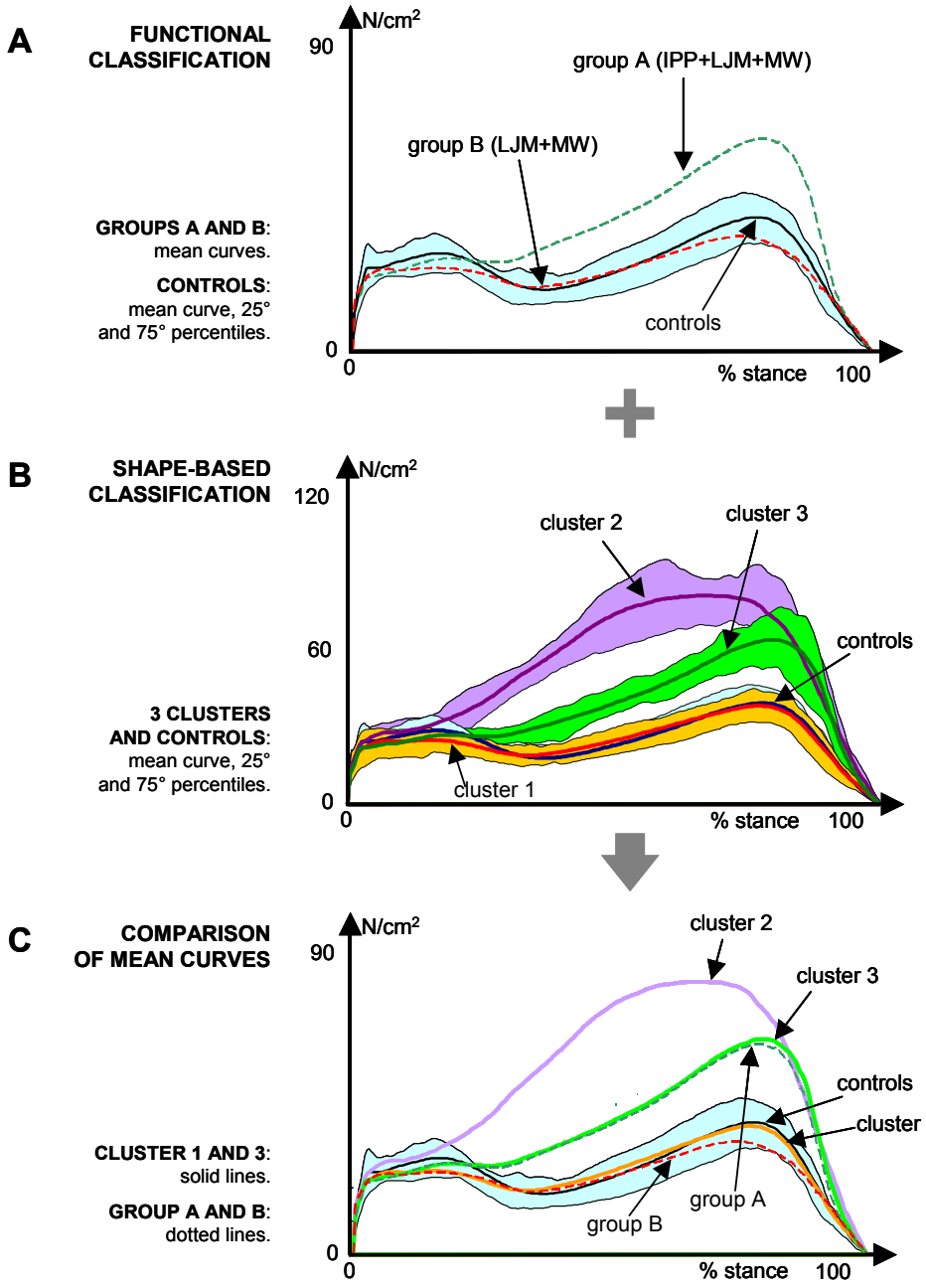

Figure 24. A. Mean curves obtained on the basis of the functional classification for group A (IPP+LJM+MW) and group B (LJM+MW). B. Results of the application of the shape-based algorithm. C. Comparison between functional and shape-based classification

Numerical data related to the two classifications are reported and compared in Table 14, where it is possible to examine the patients' spread over the three clusters defined by the K-means algorithm.

Table 13. Patients' classification based on foot-ankle functional impairments. Patients' spread over the three clusters defined by the K-means algorithm

Group	Criteria	Total	Cluster 1	Cluster 2	Cluster 3
Cases		97	53	12	32
A	IPP and LJM and MW	26	0	0	26
B	not IPP and LJM and MW	21	21	0	0
C	IPP only	9	0	3	6
D	no motor impairment	29	29	0	0
E	contra-lateral, other pathologies	12	3	9	0
Ulcerated After Test		11	0	5	6

Cluster 1 includes those patients who have not yet developed hyperpressure even though limitations in muscular strength and joint mobility at the ankle might be present. Cluster 3 well identifies those patients who are seriously impaired in terms of ankle functionality and peak pressures under the metatarsals. 6 out of 11 neuropathic patients who ulcerated few months after the test fall inside this cluster. Cluster 2 well identifies all those patients who developed abnormal loading patterns. Most of them could not be considered as "pure" diabetic neuropathic patients, since they were affected by serious concurrent diseases like orthopaedic pathologies or visual and/or acoustic impairments, or previous plantar ulcers at the contra-lateral foot. In order to verify the effectiveness of the algorithm as a test based on PPC only, its sensitivity and specificity were calculated with respect to groups A and B. With group A the algorithm showed high sensitivity and specificity (1 and 0.92, respectively); with group B it was highly sensitive but not so specific (1 and 0.58, respectively). Table 15 contains mean values, standard deviations and statistical significance ($p<0.05$) of the main clinical (VPT, NDS) and functional (IPP, MW, LJM) parameters inside each cluster and with respect to the control group. Only data acquired with the foot in neutral position and related to the sagittal plane have been considered of interest here and reported.

Table 14. Mean values, standard deviations and statistical significance ($p<0.05$) of main clinical (VPT, NDS) and functional (IPP, MW, LJM) parameters (sagittal plane and neutral position) inside each cluster and related to control group

Cluster		VPT(V)	NDS (0-12)	Pressure (N/cm^2)		Moment (Nm)*		Joint angle (°)
				rearfoot	*forefoot*	*plantar*	*dorsal*	
1	mean	13.8	3.2	28.5	41.9	46.2	34.7	64.7
	SD	11.0	3.1	9.2	9.0	14.7	12.4	13.2
	n	53	53	53	53	53	53	53
	ANOVA	*					*	*
2	mean	26.0	5.9	30.1	93.2	51.7	42.7	66.0
	SD	16.7	3.8	8.1	15.0	15.3	8.5	9.2
	n	12	12	12	12	12	12	12
	ANOVA	*	*		*			
3	mean	22.8	5.8	29.5	73.5	38.7	31.9	55.9
	SD	11.6	3.3	9.3	16.6	132.1	5.9	8.1
	n	32	32	32	32	32	32	32
	ANOVA	*	*		*	*	*	*
Controls	mean	2.0	0.0	28.9	39.6	50.6	46.7	74.6
	st dev	0.0	0.0	8.3	9.7	12.8	11.4	13.6
	n	42	42	42	42	42	42	42

* normalised with respect to BMI; moments are measured under isometric conditions (sagittal plane, neutral position)

Relationship between clinical and biomechanical variables

Table 16 reports, for both patients and controls, the mean values of the independent factors included in the model.

Table 15. Mean values and standard deviations of independent variables of patients and controls which have been included in the regressive model

Group	Cases	Age (yr)	Height (cm)	Body mass (kg)	BMI (kg/cm^2)	VPT (V)
Controls	22	50.41 (±14.6)	168.55 (±8.8)	71.00 (±11.3)	24.86 (±2.6)	-
Diabetics	60	53.97 (±12.8)	168.20 (±9.7)	76.42 (±15.6)	26.97 (±4.8)	13.00 (±8.3)

The statistical model which best fitted the biomechanical parameters of the ankle complex functionality was the Piecewise linear regression model with computer-fixed breakpoint. For any angular excursion or moment in any of the three anatomical planes, the model converged within 50 iterations. As for the control group, it succeeded in explaining more than 90% of variance. In the presence of neuropathy, the same model was applied without and with the clinical independent variable VPT. The inclusion of this variable always enhanced the percentage of explained variance but for plantar flexion moment, as reported in Table 17.

Table 17. Percentages of variance explained by Piecewise linear regression models applied to controls and patients

Parameter	Controls	Patients	
		without VPT	*with VPT*
Plantar flexion moment (Nm)	91.4	91.2	91.3
Dorsal flexion moment (Nm)	91.9	93.5	97.6
Dorsal flexion angle (°)	93.1	87.1	89.4
Plantar flexion angle (°)	98.1	91.2	96.0

Figure 25 summarises the results of the application of the piecewise model to estimate the moments generated by maximal isometric plantar and dorsal flexion (sagittal plane, neutral position) (Figure 25A), and the maximum plantar and dorsal flexion angles (sagittal plane) (Figure 25B). For patients values were estimated by using:

i) same model and same coefficients as controls (bad fitting);
ii) same model as controls but with suited coefficients (good fitting);
iii) complete model, with same independent variables as controls plus VPT (best fitting).

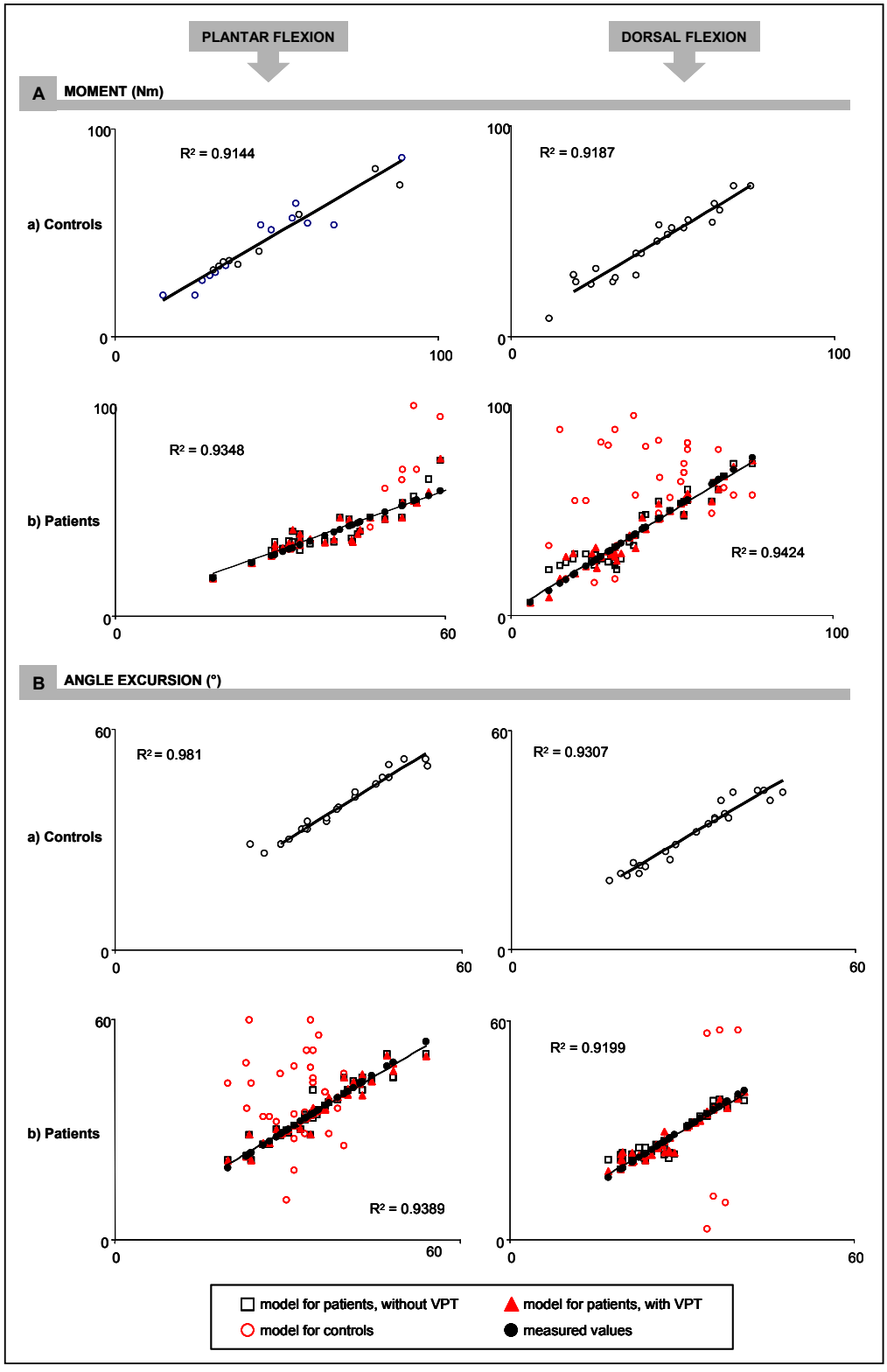

Figure 25. Results of the application of the piecewise model measured *vs* estimated values for controls (A); observed values for patients *vs* values estimated (B)

DISCUSSION

Foot-floor interaction

The analysis of the three GRF components for total foot and for the three major subareas of interest allowed the detailed description of the foot loading during different time points of the stance phase of gait. The relationships used to estimate tangential forces acting on foot subareas have been analytically deduced under simplified hypotheses. Nevertheless the following observation supports the validity of the estimation procedure.

Figure 26 reports the time courses of the vertical GRF components under the whole foot and the three analysed subareas. As it can be deduced by analysing the figure, there are time intervals in which one of the selected areas is the only (or the major) part of the foot in contact with the platform, thus the estimated local tangential forces coincide with (or are very close to) the corresponding global values measured by the force platform. Furthermore the curve patterns show no lack of continuity when passing from this condition to the following one in which more subareas are simultaneously in contact with the platform.

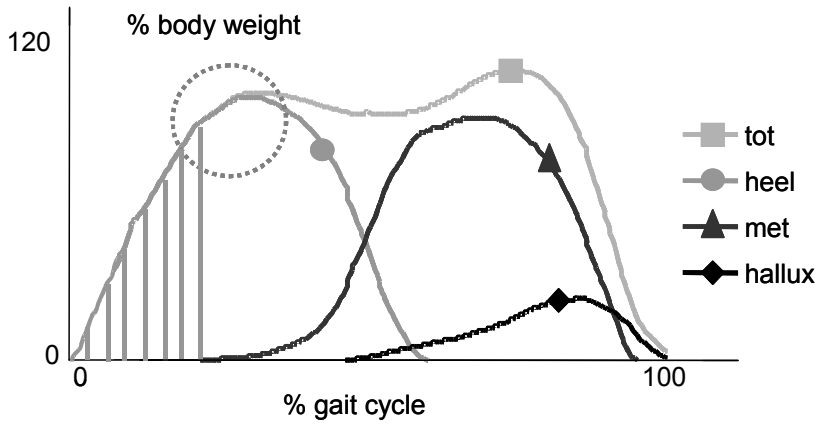

Figure 26. Time courses of the vertical GRF components under the whole foot, the heel, the metatarsals and the hallux

In agreement with previous studies (102), GRF vertical component showed a significant increase in the peak value at the metatarsal area in patients with peripheral neuropathy. Concurrently, a progressive reduction of the peak value of this component was observed at the hallux and heel areas. The reduced vertical component beneath these two sub-areas could be related to peripheral neuropathy.

A similar reduction of this component at the hallux area has been also reported by Perry (103) and Lavery (104). The reduced load at the hallux area could be explained by severe deformities of the toes (claw toe) typical of the most advanced stages of diabetic motor neuropathy (5).

Only two authors have evaluated the tangential components of GRF in diabetic patients (25-26), and both reported data related to the total foot in patients wearing shoes. In this way they tested shoe-to-floor rather than foot-to-floor interaction. In the present study, instead, forces

were evaluated under the feet of barefoot patients to better characterize the biomechanical performance of the neuropathic foot.

The anterior-posterior component of GRF is mainly expressed during the strike and the push-off phases of gait. Under the heel and hallux areas the peak value of this component was found to be significantly reduced in patients with diabetic neuropathy.

With regard to the medio-lateral GRF component, only DPU patients with previous ulceration (DPU) showed a significant increase in this component at the metatarsal area. From the data collected in this part of the study, it is not possible to establish the causes, but it could be a consequence of the peripheral neuropathy. The causative role of peripheral neuropathy could be supported by the observations that neuropathy in the DPU group was more severe than in the DN group, and that multiple correlations do exist between VPT and the medial component of the GRF. On the other hand, the increased tangential stress could be a consequence of the previous ulceration, given that healed soft tissue presents different biomechanical characteristics, such as increased hardness, that can impair elasticity (105). In any case, the existence seems reasonable of a relationship between tangential forces recorded at the metatarsals area and the occurrence of neuropathic ulcers just under the metatarsal heads, justifying the increased risk of recurrence observed in DPU patients.

Increased medio-lateral horizontal forces in diabetic neuropathic patients have been described by Mueller (106). Shaw (26) described a similar trend, but they considered this component too small to play any significant role in plantar ulceration. In addition they were doubtful about their own data because they analysed the shoe-to-floor interaction, recording only the total resultant force expressed by the whole foot. These authors considered that the question was still open to debate, awaiting for the introduction of technologies more effective at detecting tangential forces at different sites of the foot.

The equipment used in the present study allowed the measurement of the tangential force pattern expressed by different areas of the foot during foot-to-floor interaction. The increased tangential forces recorded at the metatarsal region in DPU patients suggest that they may have a role in the greater risk of recurrence observed in those patients (107).

The accurate quantification of spatial and temporal evolution of COP pattern has been proved to be effective in describing the way in which the foot manages the floor during gait.

Looking at the classes behaviour, healthy subjects show a COP progression which starts from the heel, passes through the metatarsals, reaches the anterior and medial part of the foot and stops on the hallux. This is well in agreement with the COP pattern described in (33) for healthy barefoot gait. Diabetic patients with severe neuropathy, instead, approach the floor with the most anterior part of the heel and perform their push-off phase at the metatarsals level, as it is proven by the reduction of the COP progression along the longitudinal axis.

Mueller (106,108) observed reduced ankle mobility and decreased plantar flexor strength in diabetic patients and suggested that changes in foot loading during gait may be the cause of the diminished ability of the plantar flexor muscles to push off and to generate plantar flexor moments or power during the last phase of the stance. In agreement with this hypothesis, the gait pattern resulting from the present investigation appears as a flat-footed gait, characterized by a stance-phase that involves the whole foot, with a minimal heel strike (as expressed by a reduction of the vertical and anterior-posterior component of GRF in the heel area) and a minimal push-off phase, and thus a minimal involvement of the hallux in the final phase of the stance of all the three GRF components in this area.

Neuropathic gait is also characterised by a significant reduction of the COP trajectory along the medio-lateral axis and a concurrent shift of the loading pattern from the lateral towards the medial part of the foot. According to (36), this might be read as a clear sign of instability of the whole ankle articular complex. The analysis of a COP index - calculated as the ratio between

the COP areas that are lateral and medial to the midline of the foot - allows the authors to state that the instability of a foot, when it should be stable, creates a premature medial distribution of GRF as seen by the COP pattern.

On the basis of our findings we hypothesise that limited muscular functionality at the ankle joint should be included in the causes that mainly lead to critical changes in neuropathic walking strategy. The hypothesis is well supported by the accurate analysis of the role that specific muscle compartments of the leg have in managing the floor. Andersen (109-110) demonstrated that diabetic motor neuropathy causes a distal-proximal atrophy of the muscles of the lower extremities resulting in a significant loss of function in foot and ankle muscles. This needs to be compensated by the proximal musculature of the hips and, indeed, diabetic neuropathic patients appear to pull their legs forward using hip flexor muscles (hip strategy) rather than pushing the legs forward using plantar-flexor muscles (ankle strategy) (106). Hunt (111) discussed eventual links between muscles and abnormal foot function; more specifically, he stated that between heel contact and 10% of stance, dorsiflexors act eccentrically and evertors concentrically. As the above muscle groups, especially tibialis anterior, are weak in neuropathic patients (5), they lack foot control in the heel strike phase, which entails a flat-footed approach and poor foot eversion. This in turn explains the poor lateral shift of the load also during foot flat phase, heel rise and push off, when the increased unbalance between plantar and dorsal flexors, and between invertors and evertors, greatly impairs the rise of the forefoot both in the sagittal and frontal planes. However, in diabetic patients without neuropathy, a certain degree of stiffness of the ankle joint may in addition be responsible for the reduced excursion of COP. Thus the limited joint mobility (112) could also have a role in the alteration of the walking pattern (113-114), as confirmed by the data on pure diabetic patients that were acquired during the present study.

As for the loading time, a significant increase in absolute values was found in patients with peripheral neuropathy, as reported in previous studies (25, 26). More specifically, the highest increase was recorded at the heel and metatarsal area, while loading time was significantly reduced at the hallux area. These results indicate that the increase in contact time is not homogeneous for the total foot during the stance phase. It is thus reasonable to infer that it could result not only from the loss of proprioception (115-116), but also from the hypothesised compartmental muscle weaknesses which, in the presence of neuropathy, affect ankle dorsal flexors more than other muscle compartments (5, 116).

Joint mobility and muscular functionality of the foot-ankle complex

Motor disturbances have been clinically recognised as part of the functional impairments caused by diabetic neuropathy. An interesting review has been written by Andersen and Jakobsen on motor dysfunction in diabetic neuropathic patients (117), whose main issues deserve to be reported here. Since the late 1980's, motor nerve conduction velocity (NCV) has been shown to be reduced in the presence of diabetic neuropathy, and EMG studies have demonstrated signs of denervation and compensatory reinnervation. Although these studies clearly document the existence of motor nerve dysfunction, muscle strength and EMG abnormalities have been poorly quantified so far. Only semiquantitative techniques have been used, like manual muscle testing (MMT), or simple functional tests like standing on the heel. The main reason for this lack of interest in the rigorous assessment of muscle strength stems from the Consensus Development Conference on Standardised Measures in Diabetic

Neuropathy held in 1992, where the strength of groups of muscles, rather than individual muscles, was emphasized, and therefore mechanical measurements of muscle strength were concluded to add no precision. The frequent abnormalities of the joints and periarticular tissues in diabetic patients were considered a hindrance for evaluation. However, while mechanical measurements of muscle strength were not recommended, hypotheses about the role of motor dysfunction in the pathogenesis of foot ulcers were frequently formulated and diffused. In the presence of wasted foot muscles, in fact, it is reasonable to hypothesise that the metatarsal heads become preminent, which may result in increased foot pressures. It was also reported that impaired muscle strength measured using MMT is an independent predictor of foot ulceration in patients with diabetic neuropathy.

Notwithstanding the International recommendations, the review reports about a few studies dealing with mechanical measurements of muscle strength. Most of them were based on isokinetic dynamometry, since in the clinical environment the dynamic muscle function, as reflected by isokinetic muscle strength, is considered to be an indicator of independence and well-being in the elderly. Major results were: statistically significant reduction of maximal isokinetic muscle strength at the ankle (from 21 to 45% according to the type of diabetes and the measuring techniques); minor reduction at the knee (16%); statistically insignificant reduction at the wrist (10%). Maximal isometric strength was only assessed during postural studies by using a hand-held dynamometer, and the authors reported negligible reduction at the knee, and some reduction at the ankle (21% and 18% for neuropathic and non neuropathic patients, respectively). Experimental isokinetic data partially disagreed with the theory in fashion, since neuropathic muscle weakness was believed to result in foot drop, suggesting that the ankle dorsal flexors should be more impaired than the plantar flexors. Conversely, the data showed similar degrees of weakness and atrophy of ankle dorsal and plantar flexors. The authors explained the described functional difference not as caused by selective weakness or atrophy of the ankle dorsal flexors, but rather as a consequence of the biomechanical properties of the whole ankle articular complex, probably combined with a higher capacity of the ankle plantar flexors. An important observation by Windenbank was reported in the review. He argued that isokinetic exercise, to a greater extent than isometric exercise, involved factors besides muscle strength, including an intact sensory nervous system.

From a biomechanical point of view, several experimental studies, both *in vitro* and *in vivo*, and models have been discussed up to now in the attempt of gaining deeper knowledge in the physiology of the ankle complex. Lever arms of the main flexor and extensor muscles have been studied in the sagittal plane while taking into account for the mechanical effects of the retinacula which constrain the tendons at the ankle joint. Various inclinations of ankle and subtalar axes of rotation have been calculated. Some critical issues are still questioned, dealing with the zero position of the subtalar joint, its nature of flexible joint, the movement of the whole ankle complex in the three reference planes under the effect of load, and so on. The measurement system proposed in this study is based on a fixed reference system which hardly coincide with the instantaneous anatomical reference system. This constraint could represents a limitation in the accuracy of the measurements, but at the same time it delivers accurate, overall information on the simultaneous effect of i) changing positions of the rotation axis; ii) the spanning of the tendons over several joints, and iii) action of retinacula, sheats, or bony structures influencing muscle and tendon course (118).

Ankle articular mobility and isometric muscle strength were then measured under better controlled conditions. The whole measurement system – accurately characterised both mechanically and electronically – and the associated measurement protocol showed adequate functional characteristics in terms of feasibility, reliability, robustness and repeatability. A visual feedback based on the EMG activity of two main ankle dorsal and plantar flexors greatly

helped control the initial level of muscle contraction. Torques and moments were measured with the patient seated and the loading on the foot balanced. The acquired data were then normalised with respect to BMI and referred to a standard BMI value. Median values were calculated for each class and each parameter, and non parametric tests (Mann-Whitney U test, $p<0.05$) were applied to highlight statistical differences, if any.

The assessment of the functionality of the ankle articular complex in diabetic patients, with and without peripheral neuropathy, showed a general trend towards the reduction of the range of motion in all planes of the anatomic reference system, and in both directions. The more severe the neuropathy, the greater the impairment, but, surprisingly enough, limitations were also evident in diabetic patients with NDS and/or VPT below the common neuropathic thresholds. Limitation of joint mobility was greater in the sagittal plane than in the other two planes, and in dorsal flexion more than in plantar flexion. Statistical non-parametric analysis revealed significant limitation of dorsal flexion also in D patients. This finding is important because it confirms that a certain joint stiffness occurs before neuropathy, and it cannot be simply regarded as a consequence of muscular dysfunction. DN patients showed joint mobility reduction in all planes and all directions of movement, and this is well in agreement with experimental data, previously reported in this section, related to foot-floor interaction. Increased ankle stiffness, in fact, interferes with the correct foot loading pattern during gait, and the poor inversion-eversion movement confines the progression to the sagittal plane exclusively.

A similar decreasing trend was observed with respect to the muscular functionality of the foot-ankle complex. Also in this case a major reduction was measured in correspondence with moments due to the action of ankle dorsal flexors in the sagittal plane. The reduction was greater for DN patients, but it was already present (and statistically significant) in D patients. No alteration of plantar flexors activity was found for D patients, while they produced significantly lower moments in case of severe neuropathy, but only with the foot 30° plantarflexed with respect to the shank. This finding deserves further investigation in terms of EMG, MRI or NCV tests. However, it is reasonable to hypothesise that the measured alterations could be associated with the fact that plantar flexors are hardly used under the described working conditions, as confirmed by the concurrent reduction of the range of motion in the sagittal plane. Furthermore, unaltered moments could not be in contrast with the muscle atrophy experimentally demonstrated in other studies. Neuropathic plantar flexors might indeed be weaker than those of control subjects, but other factors could influence the measured value of torque, first and foremost the modified thickness and elasticity of tendons, which in turn changes the stiffness of the whole muscle-tendon system. The study by Salsich (119) could also help in this discussion. The study reports an increased percentage of passive torque in diabetic neuropathic patients, who actually experience a reduction of active force in plantar flexors, but compensate it with the simultaneous increase of stiffness.

The mobility of the 1st metatarso-phalangeal joint was also found to be impaired, but the possible causes and effects of this finding, directly related to the alterations in the examined soft structures, will be discussed in the next paragraph.

Functionality of tendinous and ligamentous structures of the foot-ankle complex

In diabetic patients, peripheral polyneuropathy (sensory and motor) is responsible for remarkable alterations of both structure and function of the foot. Atrophy and reduced density of intrinsic muscles, tendinopathy, deformities of the internal structure such as claw toes and

prominent metatarsal heads, and denervation of tendinous and ligamentous structures have been reported in clinical observations or experimental studies (3, 20, 120-122). Also plantar soft tissue has been studied, but its changes were associated with age rather than with diabetic neuropathy (121). The role of these functional and structural changes in the development of abnormal plantar pressures has also been discussed (21).

Earlier in the present study, we discussed the alterations in plantar pressure distribution observed in diabetic patients without neuropathy, suggesting that other changes may occur before neuropathy becomes evident. Limited ankle joint mobility and reduced muscular functionality have been proved to take place at early stages of neuropathy. The hypothesis of this part of the study is that changes in the locomotor pattern may also be correlated with abnormalities of tendinous and ligamentous structures.

Increased thickness of ligamentous structures of the most distal parts of the body was observed in diabetic patients. As an example, Lundbeak highlighted the significant thickening of palmar fascia (123). Tendinopathy of hands and feet was documented too (3), but only in the presence of peripheral neuropathy.

The ultrasound examination of the patients recruited for the present study revealed an overall increase in the thickness of the main tendinous and ligamentous structures of the foot-ankle complex. Greater alterations were found for Achilles tendon and plantar fascia, more evident in the presence of neuropathy, but already present in pure diabetic patients. Thus, it seems reasonable to suggest that diabetic neuropathy may not be the only responsible condition for the pathogenesis of forefoot hyperpressure, but several factors may contribute to gait pattern alteration.

Plantar fascia, despite being a passive ligamentous structure, plays an essential role in the performance of gait. More precisely, during landing and stance it participates to force absorption at the midtarsal joint; it mainly acts as a truss, and the metatarsals undergo a compressive stress. During propulsion, it acts as a beam thus maintaining the longitudinal arch of the foot, and the metatarsals undergo a bending stress (68, 87). The following explanation aims at better clarifying these concepts.

During stance, a downward force on the talus is counteracted by an upward force on the metatarsal heads and toes and an upward force on the calcaneus (124). The upward force produces moments that tend to flatten the arch. These moments can be counteracted by the horizontal forces tending to tie the forefoot and calcaneus together. These forces are generated in the passive ligamentous plantar fascia (68, 125-126). The active contraction of intrinsic foot muscles does obviously contribute, but in the presence of neuropathy these muscles showed a certain level of atrophy, and their opposition to the flattening of the arch during gait decreased accordingly (121). On the other hand, several studies showed the role of plantar fascia in terms of arch height maintenance and forefoot loading, and the significant biomechanical consequences of its inflammation, partial resection or complete rupture (76, 79, 82, 88, 127-128).

Protein glycosilation and the consequent collagen abnormalities (129) entail greater transversal section of plantar fascia and, reasonably, greater coefficient of elasticity. Both causes lead to an increase in the resistant horizontal forces. The latter phenomenon contributes to impairing the normal adaptation of the foot to the floor in each phase of stance.

Several studies have also been conducted on the effects of Achilles tendon thickening in terms of changes in the percentages of active and passive torque of ankle plantar flexors, changes in the function of the muscle-tendon unit and in ankle stiffness, increased tensile forces at the calcaneus, increased forefoot pressures, increased resistant forces induced in plantar fascia (59-60, 119, 130-131). Some authors discussed the effect of Achilles tendon lengthening in diabetic neuropathic patients, the reduction of forefoot peak pressures, and even raised doubts about the long-term effectiveness of this surgical intervention (62-64). The measurement

conducted in the present study confirmed a significant increase in the thickness of Achilles tendon, greater for severe neuropathy, but already present in pure diabetic patients. The reasons for Achilles tendon thickening may be various; worth highlighting are the glycosilation of proteins and the effect of abnormal, cumulative stress due to changes in the walking strategy (132). Once the biomechanical link between Achilles tendon and plantar fascia has been assessed, it is reasonable to state that the increased thickness of the former structure may entail a further increase in the tensile force that the latter structure exerts at the metatarso-phalangeal joints. Once neuropathy becomes severe, toe deformities and the hyperextension of metatarso-phalangeal joints (109) further increase plantar fascia tension and maintain the foot rigid and the longitudinal arch high (68) for almost all the stance phase of gait.

The range of motion at the 1st metatarso-phalangeal joint was also observed to be reduced due to abnormalities of joint connective tissues and to the increased tension of plantar fascia. A correlation was also found between thickness of plantar fascia and limited range of motion.

As a final result of this part of the present study, it is reasonable to state that the alteration in the function of the biomechanical unit formed by Achilles tendon, plantar fascia and metatarso-phalangeal joints in the presence of diabetic neuropathy, does significantly contribute to the development of a more rigid foot. An early onset of the Windlass mechanism – forefoot pronation, calcaneous inversion and locking of the midtarsal joints – induces an early stabilising effect in the longitudinal arch of the foot, which lasts for the whole stance phase and shares in the longer, abnormal loading of the metatarsal heads.

Functional model of the diabetic foot

All the findings of the present study that are related to the analysis of foot-floor interaction show that diabetic neuropathic patients develop a “functional flat foot”. During stance, the shift of the instantaneous point of application of GRF from the rearfoot to the forefoot is faster than normal. Moreover, a wider plantar surface is instantaneously in contact with the ground, thus specific foot subareas, including metatarsal heads, remain loaded for longer percentages of stance phase. This simple functional model explains the increased pressure-time integrals under the metatarsal heads. It agrees with most experimental data, but it is unable to explain the increased vertical and medio-lateral GRF components under the same subareas, or the concurrent reduction of COP excursion along the medio-lateral axis of the foot. The model must then be improved by adding a second functional block accounting for joint mobility and muscular activity of the ankle articular complex.

In a healthy human being, helicoidal movements of the foot-ankle complex take place to transform rotational movements of the leg around the vertical axis into prono-supination movements of the foot. This, in turn, allows the best management of forces, moments and energy during landing, stance and propulsion. Limited joint mobility in all the planes of the anatomical reference system reasonably entails impairments in the performance of physiological foot-floor interaction. Greater stiffness of the ankle complex, and the consequent poor accomplishment of the requested forefoot inversion-eversion, also explain why friction increases during propulsion, in terms of the medio-lateral GRF component under the metatarsal heads. It also explains why the COP pattern remains closer to the longitudinal axis of the foot during both transfer of load from rearfoot to forefoot and propulsion. It also allows the correct interpretation of the increased vertical force under the metatarsals and the consequent high pressures, as described by Fernando (133) in a study that associates limited joint mobility with abnormal foot pressures and diabetic foot ulceration. The plantar soft tissue under the metatarsal region, in fact, experiences a greater vertical and medio-lateral stress for a longer time than

normal. The final result is a greater thinning of the fat pad for the whole phase of propulsion, up to toe-off. The reduction of medio-lateral shift of COP pattern further unbalance the loading distribution under the forefoot: therefore those small regions undergoing dangerous peak pressures are the same small areas over which the load insists from midstance up to toe-off. It is reasonable to hypothesise then that all the changes in forefoot loading described here so far, together with the daily cumulative plantar tissue stress studied by Maluf (134), do contribute to the ulceration process.

Muscular deficit of ankle dorsal flexors must be considered a further cause behind the overall change in walking strategy. The responsibility for landing control and shock absorption during the heel contact falls mostly on dorsal flexors. The altered functionality of ankle plantar flexors may worsen the muscular control in this phase, and produces abnormalities in the performance of propulsion.

This model leads to a complementary definition of diabetic neuropathic foot as a foot that has "the function of a flat foot but the structure of a rigid pes cavus". Besides limited joint mobility, limited muscular control and functional flat foot, important changes originate from the thickening of Achilles tendon and plantar fascia. These changes can be summarised as the onset of an early windlass mechanism, lasting from the very beginning of heel contact up to the end of propulsion. In a healthy foot, the windlass mechanism allows the stabilisation of the longitudinal arch of the foot during propulsion through the locking of the midtarsal joints. During heel contact and early stance phase, instead, foot joints need to be unlocked, so that the foot may absorb the forces that, applied to the talus, are exchanged between the floor and the overlying segments of the body. In the diabetic neuropathic foot this adaptation is lost: impairments in the tibia external rotation and in the corresponding internal rotation of the calcaneus concur in maintaining the midtarsal joints locked (135), metatarsal heads are abnormally loaded, little energy is stored during heel contact and insufficient energy is delivered to correctly perform propulsion (136). Limited joint mobility of the metatarso-phalangeal joints also increase tension in plantar fascia. Moreover, as well explained by Siegel through the use of accurate 3D simulation (136), the physiological dorsiflexion of the toes pulls forward the plantar fat pad under the metatarsal heads, the metatarsals move backwards and downwards, and compressive forces through the plantar fat pads increase. This means that the longer and more sustained the dorsiflexion – as in the neuropathic foot –, the longer and the higher the compression under the metatarsal heads. A further phenomenon, the development of hallux valgus, is frequently observed in neuropathic patients. When impaired, the hallux scarcely contributes to loading transmission or to the lengthening of the lever arm during the latest phase of propulsion.

The functional changes observed and described in this long discussion give rise to an overall shift of the walking strategy from an ankle strategy to a hip strategy, which calls for a smaller medio-lateral shift of COP pattern, circumscribing the progression movement to the sagittal plane (2D pendulum model). Several studies have been conducted on this change of strategy, which should be contemporarily regarded as cause and effect of the functional impairments due to diabetes and diabetic neuropathy. In fact, it seems that this strategy is naturally chosen by neuropathic patients as the most safe, pain-relieving way of walking, and some researchers demonstrated that it contributes to reducing forefoot peak pressure (2,29-30,137-139). But, on the other hand, the unusual pattern of muscle activation (140) and joint movement might entail further stiffness of ankle plantar flexors (141), thickening of Achilles tendon, and weakness of ankle dorsal flexors (142). This consequences deserve to be accurately assessed, since they might have a critical role in the development of dangerous plantar pressures and in the pathogenesis/recurrence of plantar ulcers.

Tools and models for the clinical screening of patients at risk of ulceration

Peak pressure curve

The application of a shape-based algorithm to the PPCs of Diabetic patients with mild to severe peripheral neuropathy led to the accurate definition of three, well-separate clusters. The shape of the corresponding curves seems to be strongly related to functional impairments of diabetic gait. Cluster 1 includes those patients who have not yet developed hyperpressure, though limitations in muscular strength and joint mobility at the ankle might be present. Cluster 3 well identifies those patients who are seriously impaired as for ankle functionality and peak pressures under the metatarsals. 6 out of 11 neuropathic patients who ulcerated few months after the test fall inside this cluster. Cluster 2 well identifies all those patients who developed abnormal loading patterns. Most of them could not be considered as "pure" diabetic neuropathic patients, since they were affected by serious concurrent diseases, such as orthopaedic pathologies or visual and/or acoustic impairments, or previous plantar ulcers at the contra-lateral foot.

Once correctly quantified in terms of peak timing and values, and curve integrals, PPC could be used as a reliable and effective parameter for the early detection of risk of ulceration in diabetic patients.

Relationship between clinical and biomechanical variables

The Piecewise linear regression model seems to be an effective tool to explain high percentages of variance of biomechanical variables by means of relationships among age, height, body mass, BMI. The poor fitting of the controls' model to diabetic neuropathic patients suggests that the relationships between physical and biomechanical characteristics change with respect to a normal condition when diabetic peripheral neuropathy takes place, even at an early stage. The enhanced fitting of the model when VPT is added to the set of independent variables confirms that the chosen clinical variable is suitable and necessary to explain biomechanical alterations that are typical of diabetic neuropathy.

CONCLUSIONS

The biomechanics of the diabetic neuropathic foot undergoes significant changes due to structural and functional alterations of the somatosensory, muscular, tendinous, ligamentous and bone structures of the whole foot-ankle complex.

Measurement equipments, protocols and methodologies which are typical of gait analysis were purposely set up and specialised in the present study to assess the function of the diabetic foot-ankle complex under controlled conditions, and a wide clinical investigation was then conducted on 61 diabetic patients and 21 healthy volunteers.

The analysis of the residual ability of the main functional blocks contributed to gain a deeper knowledge into the role each of them plays in the pathogenesis of plantar ulcers and to define a functional model of the diabetic neuropathic foot. It seems that none of the observed functional impairments, if acting alone, could be responsible for ulceration, but their concurrent action may reasonably take the plantar soft tissue under the forefoot into the range of "potential damage", as defined by the Physical Stress Theory (132).

When designing dedicated rehabilitation processes, aimed at preventing the onset of plantar ulcers, the assessment of the level of impairment of each functional block might result in a more effective therapy. The use of simple tools for ambulatory screening of few, meaningful parameters will be of great help in the early detection of patients at risk of ulceration, and at the same time might give preliminary indications about the functional blocks that are experiencing critical impairments.

REFERENCES

1. Barbagallo M, Novo S, Licata G, Resnick LM. Diabetes, hypertension and atherosclerosis: pathophysiological role of intracellular ions. *Int Angiol* 1993;12(4):365-70.
2. Kwon OY, Mueller MJ. Walking patterns used to reduce forefoot plantar pressures in people with diabetic neuropathies. *Phys Ther* 2001;81(2):828-35.
3. Ramirez LC, Raskin P. Diabetic foot tendinopathy: abnormalities in the flexor plantar tendons in patients with diabetes mellitus. *J Diab Comp* 1998;12:337-339.
4. Cavanagh PR, Perry JE, Ulbrecht JS, Derr JA, Pammer SE. Neuropathic diabetic patients do not have reduced variability of plantar loading during gait. *Gait and Posture* 1998;7:191-99.
5. Schoenhaus HD, Wernick E, Cohen RS. Biomechanics of the diabetic foot. In: Frykberg RG (Ed.). *The high risk foot in diabetes mellitus*. 1st ed. New York: Churchill Livingston Inc; 1991. p. 125-37.
6. Boulton AJM. Clinical presentation and management of diabetic neuropathy and foot ulceration. *Diab Med* 1991;8:S52-S57.
7. Edmons ME, Nicolaides KH, Watkins PJ. Autonomic neuropathy and diabetic foot ulceration. *Diab Med* 1986;3(1):56-59.
8. Edwing DJ, Clarke BF. Autonomic neuropathy: its diagnosis and prognosis. *Clin Endocrinol Metab* 1986;15(4):855-88.
9. Fedele D, Comi G, Coscelli C, Cucinotta D, Feldman EL, Ghirlanda G, Greene DA, Negrin P, Santeusanio F. A multicenter study on the prevalence of diabetic neuropathy in Italy. Italian Diabetic Neuropathy Committee. *Diabetes Care* 1997;20(5):836-43.
10. Greene DA, Browne MJ. Diabetic polyneuropathy. *Semin Neurol* 1987;7:18.
11. Spallone V, Tomei E, Spartera C, Sideri G, Bollea A, Laglia P, Petrassi C, Savina A, Menzinger G. Sclerosi di Monckeberg ed alterazione di flusso nella neuropatia diabetica. *Giornale Italiano di Diabetologia* 1986;6:13.
12. Uccioli L, Mancini L, Giordano A, Solini A, Magnani P, Manto A, Cotroneo P, Greco AV, Ghirlanda G. Lower limbs arterio-venous shunts, autonomic neuropathy and diabetic foot. *Diabetes Res Clin Pract* 1992;16(2):123-30.
13. Cavanagh PR, Ulbrecht JS, Caputo GM. New developments in the biomechanics of the diabetic foot. *Diabetes Metab Res Rev* 2000;16(Suppl.1):S6-S10.
14. Stokes IAF, Faris IB, Hutton WC. The neuropathic ulcer and loads on the foot in diabetic patients. *Acta Orthop Scand* 1975;46:839-47.
15. Veves A, Murray HJ, Young MJ, Boulton AJM. The risk of foot ulceration in diabetic patients with high foot pressure: a prospective study. *Diabetologia* 1992;35:660-63.
16. Katoulis EC, Boulton AJM, Raptis SA. The role of diabetic neuropathy and high plantar pressures in the pathogenesis of foot ulceration. *Horm Metab Res* 1996;28:159-64.
17. Frykberg RG, Lavery LA, Pham H, Harvey C, Harkless L, Veves A. Role of neuropathy and high foot pressures in diabetic foot ulceration. *Diabetes Care* 1998;21(10):1714-19.
18. Stess RM, Jensen SR, Mirmiran R. The role of dynamic plantar pressures in diabetic foot ulcers. *Diabetes Care* 1997;20(5):855-58.
19. Masson EA, Hay EM, Stockley I, Veves A, Betts RP, Boulton AJM. Abnormal foot pressures alone may not cause ulceration. *Diabetic Med* 1989;6:426-28.

20. Smith KE, Commean PK, Mueller MJ, Robertson DD, Pilgram T, Johnson J. Assessment of the diabetic foot using spiral computed tomography imaging and plantar pressure measurements: a technical report. *J Rehabil Res Dev* 2000;37(1):31-40.

21. Cavanagh PR, Ulbrecht JS. Biomechanics of the Diabetic Foot: A Quantitative Approach to the Assessment of Neuropathy, Deformity, and Plantar Pressure. In: Jahss MH (Ed). *Disorders of the Foot*. 3 Vol. 2nd ed. Philadelphia (PA): Saunders WB; 1991. p. 1864-1907.

22. Duckworth T, Boulton AJM, Betts RP. Plantar pressure measurements and the prevention of ulceration in the diabetic foot. *J Bone Joint Surg* 1985;67B:79-85.

23. Cavanagh PR, Simoneau GG, Ulbrecht JS. Ulceration, unsteadiness, and uncertainty: the biomechanical consequences of diabetes mellitus. *J Biomech* 1993;26(1):23-40.

24. Pollard JP, LeQuesne LP, Tappin JW. Forces under the foot. *J Biomed Eng* 1983;5:37–40.

25. Katoulis EC, Ebdon-Parry M, Lanshammar H, Vileikyte L, Kulkarni J, Boulton AJM. Gait abnormalities in diabetic neuropathy. *Diabetes Care* 1997;20(12):1904-07.

26. Shaw JE, Van Schie CHM, Carrington AL, Abbott CA, Boulton AJM. An analysis of dynamic forces transmitted through the foot in diabetic neuropathy. *Diabetes Care* 1998;21(11):1955-9.

27. Giacomozzi C, Macellari V. Piezo-dynamometric platform for a more complete analysis of foot-to-floor interaction. *IEEE Trans Rehab Eng* 1997;5(4):322-30.

28. Uccioli L, Caselli A, Giacomozzi C, Macellari V, Giurato L, Lardieri L, Menzinger G. Pattern of Abnormal Tangential Forces in the Diabetic Neuropathic Foot. *Clin Biomech* 2001;16(5):446-54.

29. Mueller MJ, Sinacore DR, Hoogstrate S, Daly L. Hip and ankle walking strategy: effect on peak plantar pressures and implications for neuropathic ulceration. *Arch Phys Med Rehabil* 1994;75:1196-1200.

30. Brown HE, Mueller MJ. A "step-to" gait decreases pressures on the forefoot. *J Orthop Sports Phys Ther* 1998;28(3):139-45.

31. Cavanagh PR. A technique for averaging center of pressure parts from a force platform. *J Biomech* 1978;11:487-91.

32. Grundy M, Blackburn M, Tosh PA, McLeish RD, Smidt L. An investigation of the centers of pressure under the foot while walking. *J Bone Joint Surg Br* 1975;57:98-103.

33. Xu H, Akai M, Kakurai S, Yokota K, Kaneko H. Effect of shoe modifications on center of pressure and in-shoe plantar pressures. *Am J Phys Med Rehabil* 1999;78(6):516-24.

34. Cornwall MW, McPoil TG. Velocity of the center of pressure during walking. *J Am Pod Med Assoc* 2000;90(7):334-38.

35. Motriuk HU, Nigg BM. A technique for normalizing centre of pressure paths. *J Biomech* 1990;23(9):927-932.

36. Scherer PR, Sobiesk GA. The center of pressure index in the evaluation of foot orthoses in shoes. *Clin Podiatr Med Surg* 1994;11(2):355-63.

37. McPoil TG, Cornwall MW. Variability of the center of pressure pattern integral during walking. *J Am Pod Med Ass* 1998;88(6):259-67.

38. Giacomozzi C, Caselli A, Macellari V, Giurato L, Lardieri L, Uccioli L. Walking strategy in Diabetic patients with Peripheral Neuropathy. *Diabetes Care* 2002;25(8):1451-1457.

39. Procter P, Paul JP. Ankle joint biomechanics. *J Biomech* 1982;15(9):627-34.

40. Wynarsky GT, Greenwald AS. Mathematical model of the human ankle joint. *J Biomech* 1983;16(4):241-51.

41. Dul J, Johnson GE. A kinematic model of the human ankle. *J Biomed Eng* 1985;7:137-43.

42. Inman VT. *The joints of the ankle*. Baltimore: Williams & Wilkins; 1976.

43. Scott SH, Winter DA. Biomechanical model of the human foot: kinematics and kinetics during the stance phase of walking. *J Biomech* 1993;26(9):1091-104.

44. Leardini A. *Geometry and mechanics of the human ankle complex, and ankle prosthesis design*. PhD Thesis. Oxford: Oxford University; 2000.

45. Manter JT. Movements of the subtalar and transverse tarsal joints. *Anat Rec* 1941;80:397-410.

46. Isman RE, Inman VT. Anthropometric studies of the human foot and ankle, eometry and mechanics of the human ankle complex, and ankle prosthesis design. *Bull Prosthet Res* 1969;10-11:97-129.

47. Sangeorzan BJ, Sidles JA. Hinge like motion of the ankle and subtalar articulations. *Orthop Trans* 1995;19(2):331-32.

48. Huson A. Mechanics of joints. *Int J Sports Med* 1984;5:83-7.

49. Olerud C, Rosendhal Y. Torsion-transmitting properties of the hindfoot. *Clin Orthop* 1987;214:285-94.

50. Engsberg JR, Andrews JG. Kinematic analysis of the talocalcaneal talocrural joint during running support. *Med Sci Sports Exerc* 1987;19:275-84.

51. Leardini A. Geometry and mechanics of the human ankle complex and ankle prosthesis design. *Clin Biomech* 2001;16(8):706-9.

52. Lundberg A. Kinematics of the ankle and foot – *In vivo* roentgen stereophotogrammetry (Review). *Acta Orthop Scand Suppl* 1989;233:1-24.

53. Lundberg A, Svensson OK, Nemeth G, Selvik G. The axis of rotation of the ankle joint. *J Bone Joint Surg* 1989;71-B(1):94-99.

54. Siegler S, Chen J, Scheck CD. The three-dimensional kinematics and flexibility characteristics of the human ankle and subtalar joint. *J Biomech Eng* 1988;110:364-85.

55. Engsberg JR. A biomechanical analysis of the talocalcaneal joint – *in vitro*. *J Biomech* 1987;20(4):429-42.

56. Elftman H. The transverse tarsal joint and its control. *Clin Orthop* 1960;16:41-5.

57. Giacomozzi C, Cesinaro S, Basile F, De Angelis G, Giansanti D, Maccioni G, Masci E, Panella A, Paolizzi M, Torre M, Valentini P, Macellari V. A measurement device for the ankle joint kinematic and dynamic characterisation. *Med Biol Eng Comput* 2003;in press.

58. Delbridge L, Ellis CS, Robertson K. Nonenzymatic glycosylation of keratin from the stratum corneum of the diabetic foot. *Br J Dermatol* 1985;112:547-54.

59. Carlson RE, Fleming LL, Hutton WC. The biomechanical relationship between the Tendoachilles, plantar fascia and metatarsophalangeal joint dorsiflexion angle. *Foot Ankle Int* 2000;21(1):18-25.

60. Snow SW, Bohne WHO, DiCarlo E, Chang VK. Anatomy of the Achilles tendon and plantar fascia in relation to the calcaneus in various age groups. *Foot Ankle Int* 1995;16(7):418-21.

61. Grant WP, Sullivan R, Sonenshine DE, Adam M, Slusser JH, Carson KA, Vinik AI. Electron microscopic investigation of the effects of diabetes mellitus on the Achilles tendon. *J Foot Ankle Surg* 1997;36(4):272-8.

62. Armstrong DG, Stacpoole-Shea S, Nguyen H, Harkless LB. Lengthening of the Achilles tendon in Diabetic patients who are at high risk for ulceration of the foot. *J Bone Joint Surg* 1999;81-A(4):535-38.

63. Hastings MK, Mueller MJ, Sinacore DR, Salsich GB, Engsberg JR, Johnson JE. Effects of a tendo-Achilles lengthening procedure on muscle function and gait characteristics in a patient with diabetes mellitus. *J Orthop Sports Phys Ther* 2000;30(2):85-90.

64. Mueller MJ, Maluf K, Sinacore DR, Hastings M, Strube MJ, Engsberg J, Johnson JE. Effect of tendo Achilles lengthening on forefoot plantar pressures, ankle motion and plantar flexor power during walking in subjects with diabetes and peripheral neuropathy: a prospective controlled clinical trial. In: *Proceedings of the 8th EMED Scientific Meeting. Kananaskis.* Alberta (Canada), July 31st – August 3rd, 2002. p. 25.

65. Thibodeau GA, Patton KT. *Anatomy and physiology*. International Edition. 2nd ed. St Louis: Mosby; 1993.

66. McMinn RMH, Gaddum-Rose P, Hutchings RT, Logan BM. *Functional and clinical anatomy*. St Louis: Mosby; 1995.

67. Maganaris CN. Tensile properties of *in vivo* human tendinous tissue. (ASB post-doctoral young investigator award 2001). *J Biomech* 2002;35:1019-27.

68. Hicks JH. The mechanics of the foot. II. The plantar aponeurosis and the arch. *J Anat* 1954;88:25-30.

69. Hicks JH. The mechanics of the foot. IV. The action of muscles on the foot in standing. *Acta Anat* 1957;27:180-92.

70. Hicks JH. The mechanics of the foot. I. The joints. *J Anat* 1954;88:25.

71. Hicks JH. The mechanics of the foot. III. The font as a support. *Acta Anat* 1955;25:34-45.

72. Mann RA, Inmann VT. Phasic activity of intrinsic muscles of the foot. *J Bone Joint Surg* 1964;46A:469-81.

73. Hamel AJ, Donahue SW, Sharkey NA. Contributions of active and passive toe flexion to forefoot loading. *Clin Orthop* 2001;393:326-34.

74. Morton DL. *The Human foot. Its evolution, physiology and fuctional disorders*. New York: Columbia University Press; 1995.

75. Perry J. Gait Anatomy and biomechanics of the hindfoot. *Clin Orthop* 1983;177:9-15.

76. Arangio GA, Xiao D, Salathé EP. Biomechanical study of stress in the fifth metatarsal. *Clin Biomech* 1997;12(3):160-64.

77. Arangio GA, Phillippy DC, Dayan Xiao, Wei-Kai Gu, Salathè EP. Subtalar Pronation – Relationship to the medial longitudinal arch loading in the normal foot. *Foot Ankle Int* 2000;21(3):216-20.

78. Wangdo K, Voloshin AS. Role of plantar fascia in the load bearing capacity of the human foot. *J Biomech* 1995;28(9):1025-33.

79. Arangio GA, Chaorong Chen, Salathè EP. Effect of varying arch height with and without the plantar fascia on the mechanical properties of the foot. *Foot Ankle Int* 1998;19(10):705-9.

80. Sharkey NA, Ferris L, Donahue SW. Biomechanical consequences of plantar fascia release or rupture during gait. Part I – disruptions in longitudinal arch conformation. *Foot Ankle Int* 1998;19(12):812-20.

81. Sharkey NA, Donahue SW, Ferris L. Biomechanical consequences of plantar fascia release or rupture during gait. Part II: alterations in forefoot loading. *Foot Ankle Int* 1999;20(2):86-96.

82. Arangio GA, Chaorong Chen, Wangdo Kim. Effect of cutting the plantar fascia on mechanical properties of the foot. *Clin Orthop* 1997;339:227-31.

83. Murphy GA, Pneumaticos SG, Kamaric E, Noble PC, Trevino SG, Baxter DE. Biomechanical consequences of sequential plantar fascia release. *Foot Ankle Int* 1998;19(3):149-52.

84. D'Ambrogi E, Giurato L, D'Agostino MA, Giacomozzi C, Macellari V, Caselli A, Uccioli L. Contribution of plantar fascia to the increased forefoot pressures in diabetic patients. *Diabetes Care* 2003;26(5):1525-9.

85. Hartigan JA, Wong MA. A k-means clustering algorithm. *Applied Statistics* 1979;28:100-8.

86. Allard P, Stokes IAF, Salathè EP, An KN. Modelling of the foot and ankle. In: Jahss MH (Ed). *Disorders of the foot and ankle*. Vol 1. 2nd ed. Philadelphia: WB Saunders; 1992. p. 432-68.

87. Salathé EP Jr, Arangio GA, Salathé EP. A biomechanical model of the foot. *J Biomech* 1986;19(12):989-1001.

88. Salathè EP Jr, Arangio GA, Salathè EP. The foot as a shock absorber. *J Biomech* 1990;23(7):655-59.

89. Boulton AJM, Kubrusly D, Bowser JH, Gadia MT, Quintero L, Becker DM, Skyler JS, Sonsenko JM. Impaired vibratory perception and diabetic foot ulceration. *Diabetic Med* 1986;3:335-37.

90. Young MJ, Boulton AJM, Mac Leod AF, Williams DRR, Sonksen PH. A multicentre study of the prevalence of diabetic peripheral neuropathy in the United Kingdom Hospital Clinic Population. *Diabetologia* 1993;36:150-4.

91. Abuzzahab FS, Harris GF, Kidder SM, Johnson JE. A kinetic, biomechanical model of the foot and ankle. In: *Proceedings of the 16th Annual International Conference of IEEE Engineering in Medicine & Biology Society*. Baltimore (USA), November 3-6, 1994. paper n. 687.

92. Abuzzahab FS, Harris GF, Kidder SM, Johnson JE. Analysis of foot and ankle kinetics during gait. In: *Proceedings of the 17th Annual International Conference of IEEE Engineering in Medicine & Biology Society*. Montreal (Canada), September 20-23, 1995. p. 732-33.

93. Gage JR. Gait analysis: an essential tool in the treatment of cerebral palsy. *Clin Orthop* 1993;288:126-34.

94. Akhlaghi F, Pepper MG. In-shoe biaxial shear force measurement: the Kent shear system. *Med Biol Eng Comput* 1996;34:315-7.

95. Macellari V, Giacomozzi C. Multistep pressure platform as a stand-alone system for gait assessment. *Med Biol Eng Comput* 1996;34:299-304.

96. Barnett S. International protocol guidelines for plantar pressure measurement. *The diabetic foot* 1998;1(4):137-40.

97. Terminology. In: University of Strathclyde, Bioengineering Unit (Ed). *Terminology and units*. *Deliverable n.4 of the C.E.C. Programme AIM, Project A-2002 CAMARC II*. Strathclyde (UK); 1994. p. 12-6.

98. Lundberg A, Goldie I, Kalin B, Selvik G. Kinematics of the ankle/foot complex: Plantarflexion and dorsiflexion. *Foot Ankle* 1989;9(4):194-200.

99. Asada H, Slotine JJE. *Robot analysis and control*. New York: J. Wiley; 1986.

100. Belfiore NP, Macellari V, Giacomozzi C, Panella A, Paolizzi M. Identificazione delle caratteristiche di funzionalità del complesso articolare della caviglia tramite robot di misura dedicati. In: DiPrampero PE, Pascolo PB (Ed). *Meccanica della locomozione e del gesto, atti 1997-1999*. Udine: Pubblicazioni CISM; 2002. p. 205-8.

101. Bobbert MF, van Ingen Schenau GJ. Isokinetic plantar flexion: experimental results and model calculations. *J Biomech* 1990;23(2):105-19.

102. Cterctecko GC, Dhanendron M, Hutton WC, Le Quesne LP. Vertical forces acting on the feet of diabetic patients with neuropathic ulceration. *Br J Surg* 1981;68:608-14.

103. Perry J, Ulbrecht JS, Derr JA, Cavanagh PR. The use of running shoes to reduce plantar pressures in patients who have diabetes. *J Bone Joint Surg* 1995;77(12):1819-28.

104. Lavery LA, Vela SA, Fleishli JG, Armstrong DG, Lavery DC. Reducing plantar pressure in the neuropathic foot. *Diabetes Care* 1997;20(11):1706-10.

105. Brink T. Induration of the diabetic foot pad: another risk factor for recurrent neuropathic ulcers. *Biomed Tech Berl* 1995;40(7-8):205-9.

106. Mueller JM, Minor SD, Sahrmann SA, Schaaf JA, Strube MJ. Differences in the gait characteristics of patients with diabetes and peripheral neuropathy compared with age-matched controls. *Phys Ther* 1994;74(4):299-308.

107. Helm PA, Walker SC, Pullium GF. Recurrence of neuropathic ulceration following healing in total contact cast. *Arch Phys Med Rehabil* 1991;72(11):967-70.

108. Mueller MJ, Minor SD, Schaaf JA, Strube MJ, Sahrmann SA. Relationship of Plantar-Flexor Peak Torque and Dorsiflexion Range of Motion to Kinetic Variables During Walking. *Phys Ther* 1995;75(8):684-93.

109. Andersen H, Gadeberg PC, Brock B, Jakobsen J. Muscular atrophy in diabetic neuropathy: a stereological magnetic resonance imaging study. *Diabetologia* 1997;40:1062-9.

110. Andersen H, Poulsen PL, Mogensen CE, Jakobsen J. Isokinetic Muscle Strenght in Long-Term IDDM Patients in Relation to Diabetic Complications. *Diabetes* 1996;45:440-5.

111. Hunt AE, Smith RM, Torode M. Extrinsic muscle activity, foot motion and ankle joint moments during the stance phase of walking. *Foot Ankle Int* 2001;22(1):31-41.

112. Andersen H, Mogensen PH. Disordered mobility of large joints in association with neuropathy in patients with long-standing insulin-dependent diabetes mellitus. *Diabetic Med* 1997;14:221-27.

113. Uccioli L, Giacomini P, Monticone G, Magrini A, Durola L, Bruna E, Parisi L, Di Girolamo S, Menzinger G. Body Sway in Diabetic Neuropathy. *Diabetes Care* 1995;18:339-44.

114. Giacomini PG, Bruno E, Monticone G. Di Girolamo S, Magrini A, Parisi L, Menzinger G, Uccioli L. Postural re-arrangement in IDDM patients with peripheral neuropathy. *Diabetes Care* 1996;19:372-4.

115. Gandevia SC, Macefield G, Burke D, McKenzie DK. Voluntary activation of human motor axons in the absence of muscle afferent feedback. The control of the deafferented hand. *Brain* 1993;113:563-81.

116. van Deursen RW, Sauchez MM, Ulbrecht JS, Cavanagh PR. The role of muscle spindles in ankle movement perception in human subjects with diabetic neuropathy. *Exp Brain Res* 1998;120(1):1–8.

117. Andersen H, Jakobsen J. Motor function in diabetes. *Diabetes Reviews* 1999;7(4):326-41.

118. Leardini A, O'Connor JJ. A model for lever-arm length calculation of the flexor and extensor muscles at the ankle. *Gait and Posture* 2002;15:220-9.

119. Salsich GB, Brown M, Mueller MJ. Relationships between plantar flexor muscle stiffness, strength, and range of motion in subjects with diabetes-peripheral neuropathy compared to age-matched controls. *J Orthop Sports Phys Ther* 2000;30(8):473-83.

120. Morag E, Cavanagh PR. Structural and functional predictors of regional peak pressures under the foot during walking. (ISB Keynote Paper – 1997). *J Biomech* 1999;32:359-70.

121. Robertson DD, Mueller MJ, Smith KE, Commean PK, Pilgram T, Johnson JE. Structural changes in the forefoot of individuals with diabetes and a prior plantar ulcer. *J Bone Joint Surg Am* 2002;84-A(8):1395-404.

122. Ackermann PW, Li J, Finn A, Ahmed M, Kreicbergs A. Autonomic innervation of tendons, ligaments and joint capsules. A morphologic and quantitative study in the rat. *J Orthop Res* 2001;19:372-8.

123. Lundbeak K. Stiff hands in long term diabetes. *Acta Med Scand* 1957;158:447-51.

124. Chapter 4: On the movement of the foot and the forces acting on it. In: Braune W, Fisher O. *The human gait*. Berlin (Germany): Springer-Verlag; 1987. p. 255-75.

125. Frankel VH. *Basic biomechanics of the skeletal system*. Philadelphia: Lea e Febiger; 1986.

126. Ker RF, Bennet MB, Bibby SR, Kester RC, Alexander RM. The spring in the arch of the human foot. *Nature* 1987;325:147-9.

127. Jacob HAC. Forces acting in the forefoot during normal gait – an estimate. *Clin Biomech* 2001;16:783-92.

128. Kibler WB, Goldberg C, Chandler TJ. Functional biomechanical deficits in running athletes with plantar fasciitis. *Am J Sports Med* 1991;19(1):66-71.

129. Crisp AJ, Heatcoate JG. Connettive tissue abnormalities in diabetes mellitus. *J R Coll Physicians Lond* 1984;18:132-40.

130. Hawkins D, Hull ML. A method for determining lower extremity muscle-tendon lengths during flexion-extension movements. *J Biomech* 1990;23(5):487-94.

131. Salsich GB, Mueller MJ, Sahrmann SA. Passive ankle stiffness in subjects with diabetes and peripheral neuropathy versus an age-matched comparison group. *Phys Ther* 2000;80(4):352-62.

132. Mueller MJ, Maluf KS. Tissue adaptation to physical stress: a proposed "Physical Stress Theory" to guide physical therapist practice, education, and research. *Phys Ther* 2002;82(4):383-403.

133. Fernando DJS, Masson EA, Veves A, Boulton AJM. Relationship of limited joint mobility to abnormal foot pressure and diabetic foot ulceration. *Diabetes Care* 1991;14(1):8-11.

134. Maluf K, Mueller MJ. Comparison of physical activity and cumulative plantar tissue stress among subjects with and without diabetes mellitus and a history of recurrent plantar ulcers. In: *Proceedings of the 8th EMED Scientific Meeting. Kananaskis.* Alberta (Canada), July 31st - August 3rd, 2002. p. 29.

135. Lundberg A, Svensson OK, Bylund C, Selvik G. Kinematics of the ankle/foot complex – Part 3: Influence of leg rotation. *Foot Ankle* 1989;9(6):304-9.

136. Lohmann Siegel K, Kepple TM, Caldwell GE. Improved agreement of foot segmental power and rate of energy change during gait: inclusion of distal power terms and use of three-dimensional models. *J Biomech* 1996;29(6):823-7.

137. Mueller MJ, Salsich GB, Strube MJ. Functional limitations in patients with diabetes and transmetatarsal amputations. *Phys Ther* 1997;77(9):937-43.

138. Mueller MJ, Salsich GB, Bastian AJ. Differences in the gait characteristics of people with diabetes and transmetatarsal amputation compared with age-matched controls. *Gait Posture* 1998;7(3):200-6.

139. Mueller MJ, Strube MJ. Therapeutic footwear: enhanced function in people with diabetes and transmetatarsal amputation. *Arch Phys Med Rehabil* 1997;78(9):952-6.

140. McNitt-Gray JL, Hester DME, Mathiyakom W, Munkasy BA. Mechanical demand and multijoint control during landing depend on orientation of the body segments relative to the reaction force. *J Biomech* 2001;34:1471-82.

141. Wright IC, Neptune RR, van den Bogert AJ, Nigg BM. The influence of foot positioning on ankle sprains. J Biomech 2000;33:513-9.

142. Weist R, Rosenbaum D. Changes of plantar pressure and muscle activity patterns under the influence of fatigue after exausting treadmill running. In: *Proceedings of the 8th EMED Scientific Meeting. Kananaskis.* Alberta (Canada), July 31st - August 3rd, 2002. p. 55.

GLOSSARY

The terminology adopted in the present study has been approved by the International Society of Biomechanics (ISB) and published in 2002 in the first part of ISB recommendation on definitions of Joint Coordinate System (JCS) of various joints for the reporting of human joint motion.[1] Definition related to the ankle-joint complex are related in the following.

Articulations

The ankle joint complex is composed of the talocrural and the subtalar joints.

- The ankle (talocrural) joint: The articulation formed between the talus and the tibia/fibula.
- The subtalar (talocalcaneal) joint: The articulation between the talus and the calcaneus.
- The ankle joint complex: The structure composed of the ankle and the subtalar joints.

Landmarks

MM: Tip of the medial malleolus.
LM: Tip of the lateral malleolus.
MC: The most medial point on the border of the medial tibial condyle.
LC: The most lateral point on the border of the lateral tibial condyle.
TT: Tibial tuberosity.
IM: The inter-malleolar point located midway between MM and LM.
IC: The inter-condylar point located midway between the MC and LC.

Planes of the tibia/fibula

Frontal plane: The plane containing points IM, MC and LC.
Torsional plane: The plane containing points IC, MM and LM.
Sagittal plane: The plane perpendicular to the frontal plane and containing the long axis of the tibia/fibula (the line connecting points IC and IM).
Transverse plane: The mutual plane perpendicular to the frontal and sagittal planes.

Reference neutral configuration of the ankle joint complex

Neutral dorsiflexion/plantarflexion: Zero degrees between the long axis of the tibia/fibula and the line perpendicular to the plantar aspect of the foot projected onto the sagittal plane of the tibia/fibula.
Neutral inversion/eversion: Zero degrees between the long axis of the tibia/fibula and the line perpendicular to the plantar aspect of the foot projected onto the frontal plane of the tibia/fibula.

[1] Wu G, Siegler S, Allard P, Kirtley C, Leardini A, Rosenbaum D, Whittle M, D'Lima DD, Cristofolini L, Witte H, Schmid O, Stokes I. ISB recommendation on definitions of joint coordinate system of various joints for the reporting of human joint motion – part I: ankle, hip, and spine. (Letter to the Editor). *J Biomech* 2002;35:543-8.

Neutral internal/external rotation:	Zero degrees between the line perpendicular to the frontal plane of the tibia/fibula and the long axis of the second metatarsal, projected onto the transverse plane of the tibia/fibula.

Reference systems and motion

Calcaneus coordinate system – xyz

- o: The origin coincident with that of the tibia/fibula coordinate system (O) in the neutral configuration.
- y: The line coincident with the long axis of the tibia/fibula in the neutral configuration, and pointing cranially.
- x: The line perpendicular to the frontal plane of the tibia/fibula in the neutral configuration, and pointing anteriorly.
- z: The common line perpendicular to x- and y- axis.

Fibula/tibia coordinate system – XYZ

- O: The origin coincident with IM.
- Z: The line connecting MM and LM, and pointing to the right.
- X: The line perpendicular to the torsional plane of the tibia/fibula, and pointing anteriorly.
- Y: The common line perpendicular to X- and Z- axis.

Motion for the ankle complex

- e1: The axis fixed to the tibia/fibula and coincident with the Z- axis of the tibia/fibula coordinate system.
  Rotation (α): dorsiflexion (positive) or plantarflexion (negative).
  Displacement (q1): medial (negative) or lateral (positive) shift.
- e3: The axis fixed to the calcaneus and coincident with the y-axis of the calcaneal coordinate system.
  Rotation (γ): internal rotation (positive) or external rotation (negative).
  Displacement (q3): correspond to compression (positive) or distraction (negative).
- e2: The floating axis, the common axis perpendicular to e1 and e3.
  Rotation (β): inversion (positive) or eversion (negative).
  Displacement (q2): anterior (positive) or posterior (negative) drawer.

Stampato da Ditta Grafiche Chicca & C. snc
Via di Villa Braschi 143, 00019 Tivoli (Roma)

Roma, dicembre 2003 (n. 4) 2° Suppl.